

Using ASTER and geophysical mapping for mineral exploration in the Wagga Wagga and Cobar areas, N.S.W.

Abstract

This study evaluated and validated (ground truthed) recently released ASTER satellite geoscience maps of Australia and evaluate their use in geological mapping within New South Wales. The Wagga Wagga 1:100 000 and the Cobar 1:250 000 map sheet areas were chosen for the study.

Most of the study focussed on Wagga Wagga, central to a new geological mapping project area of the Geological Survey of New South Wales. It included processing, interpretation and data integration with aeromagnetic and radioelement data, digital elevation data and geological data. All data were incorporated into a GIS platform to examine vegetation and regolith/soil spectral issues — in order to assess the potential for local geological/alteration models and to generate spectral–geophysical anomalies of interest. Through topographic modelling of slope information from SRTM data, techniques were developed to target terrain with greatest geological exposure and exclude areas of vegetation, active cultivation and transported cover. This included illuminating (elevation and azimuth) the SRTM data to simulate similar conditions when the relevant ASTER imagery was acquired. This was followed by field validation, using a portable field spectrometer to measure spectral signatures of outcrop and soils and to examine their comparison with the ASTER data. As the original ASTER satellite imagery can sometimes exhibit mis-calibration in areas of deep shadow and dark ground surfaces, the fieldwork demonstrated the importance of validating spectral signatures of anomalous mineralised areas.

Applying ASTER maps to the investigation of semi-arid environments, such as the Cobar region, shows the usefulness of AIOH (e.g. muscovite, illite), ferric oxide (e.g. hematite, goethite) and silica (e.g. quartz) index products in regolith mapping. When combined with radioelement K, the ASTER imagery can potentially discriminate zones of weathered regolith and exposed outcrops, thereby assisting exploration for mineralisation.

Key words: *Wagga Wagga, Cobar, ASTER, mineralogy, geophysics, DEMs, data integration*

AUTHORS

Robert Hewson,

School of Mathematical & Geospatial Sciences, RMIT University

David Robson,

*Geological Survey of New South Wales,
516 High Street, Maitland, NSW 2320*

© State of New South Wales through Department of Trade and Investment, Regional Infrastructure and Services 2014.

Papers in Quarterly Notes are subject to external review. External reviewer for this issue was Simon Oliver of Geoscience Australia. His assistance is appreciated.

Quarterly Notes is published to give wide circulation to results of studies in the Geological Survey of New South Wales. Papers are also welcome that arise from team studies with external researchers.

Contact: simone.meakin@trade.nsw.gov.au

ISSN 0155-3410



Contents

Abstract	1
Introduction	2
ASTER Multispectral Satellite Sensor	2
Mineral detection using ASTER	3
Past ASTER case studies	3
CSIRO–GA Australian ASTER geoscience map products	4
Case study areas — environment and geology	5
ASTER coverage of NSW	5
Wagga Wagga 1:100 000 map sheet area	6
Cobar 1:250 000 map sheet area	6
Datasets and methodologies	7
ASTER	7
Airborne geophysics	7
Digital elevation models (DEMs)	7
Auscover fractional landcover	8
Data integration strategies	9
Field studies and sample spectroscopy	9
ASTER validation study	10
Results	12
Wagga Wagga 1:100 000 map sheet area	12
Cobar 1:100 000 and Canbelego 1:100 000 map sheet areas	21
Conclusions	24
Acknowledgements	25
References	25

Technical editing: Richard Facer

Production co-ordination and general editing: Simone Meakin and Geneve Cox

Geospatial information: Kate Holdsworth and Nicole Edwards

Layout: Nicole Edwards

Photographs: Robert Hewson

Cover image: View southwards from the summit of The Rock Nature Reserve, near Wagga Wagga.



Trade & Investment
Resources & Energy

Disclaimer

The information (and links) contained in this publication is based on knowledge and understanding at the time of writing (February, 2014). However, because of advances in knowledge, users are reminded of the need to ensure that the information upon which they rely is up to date and to check the currency of the information with the appropriate officer of the Department of Trade and Investment, Regional Infrastructure and Services or the user's independent adviser. The product trade names in this publication are supplied on the understanding that no preference between equivalent products is intended and that the inclusion of a product name does not imply endorsement by the department over any equivalent product from another manufacturer.

Copyright

© State of New South Wales through Department of Trade and Investment, Regional Infrastructure and Services 2014. You may copy, distribute and otherwise freely deal with this publication for any purpose, provided that you attribute the Department of Trade and Investment, Regional Infrastructure and Services as the owner.

Introduction

In August 2012 a series of 17 compositional Australia-wide map products was released by the Commonwealth Scientific Industrial Research Organisation (CSIRO) and Geoscience Australia (GA) from imagery obtained by the multispectral satellite sensor, Advanced Spaceborne Thermal Emission Reflectance Radiometer (ASTER) (Cudahy 2012). This followed many successful years of data acquisition by ASTER following its development by Japan's Ministry of Economy, Trade and Industry (METI) and launch by *National Aeronautics and Space Administration* (NASA) (Yamaguchi et al. 2001). These compositional maps offer the opportunity of new 'eyes' for regional geological mapping within Australia to assist exploration activities.

This particular study aims to examine and compare the application of the Australian ASTER map products within two different environments of New South Wales (NSW), encompassing the temperate and cultivated Wagga Wagga 1:100 000 (100K) and semi-arid Cobar 1:250 000 (250K) map sheet areas. Wagga Wagga was examined in particular in conjunction with traditional airborne magnetic, radiometric, and digital elevation model (DEM) datasets acquired by the Geological Survey of New South Wales (GSNSW). An overall objective was to examine the robustness of geoscience mapping capabilities of ASTER, as individual map products, and via data integration, within different environments of NSW. This study also follows the previous presentation at the 2013 Australian Society of Exploration Geophysicists conference (Hewson et al. 2013). A more detailed description of this study is found in Hewson (2013).

ASTER multispectral satellite sensor

ASTER acquires imagery within a 60 km x 60 km scene area from 14 different spectral bands with a pixel resolution of between 15 m and 90 m, depending on whether they were generated by the Visible–Near Infrared (VNIR), Shortwave Infrared (SWIR) or Thermal Infrared (TIR) sensors (Yamaguchi et al. 2001).

ASTER tracks a similar Earth orbit and altitude to the older Landsat TM satellites, with similar VNIR bands (minus band 1) but with five additional SWIR bands, providing higher spectral resolution than Landsat TM's band 7 (Figure 1). ASTER also measures radiance using five bands within the TIR wavelength region (8–12 μm) (Figure 1) providing the first access to civilian multispectral TIR data at moderate spatial resolution (90 m).

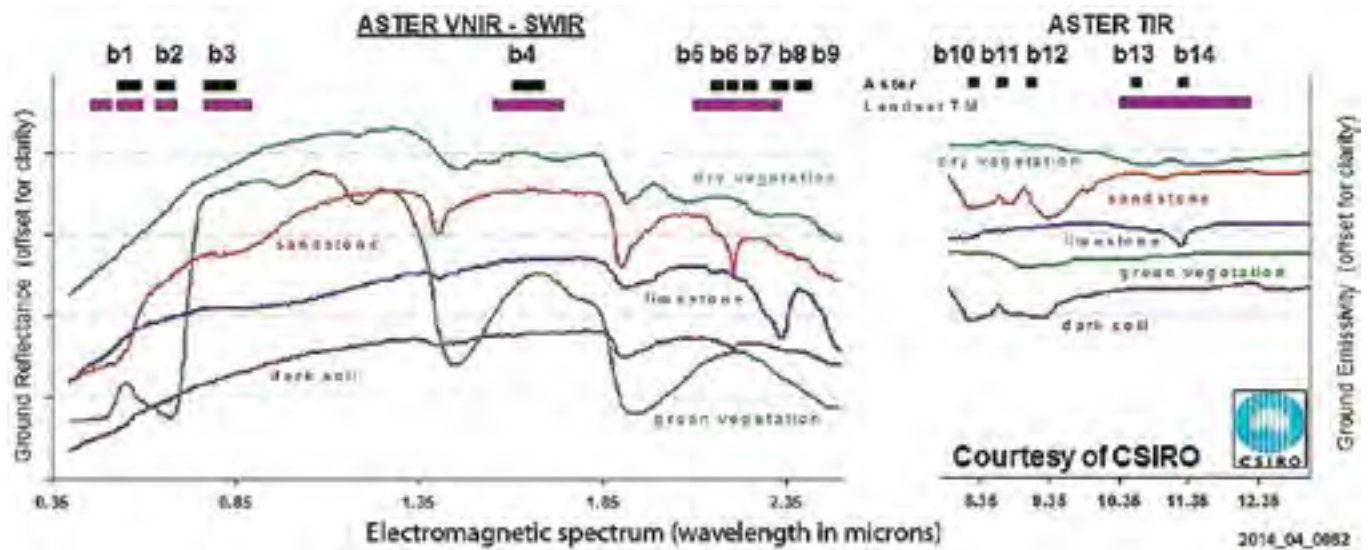


Figure 1. Typical reflectance and emissivity signatures and their comparison with ASTER and Landsat TM spectral bands (e.g. bands : 'bx'). Note: 1 μm \equiv 1000 nm.

The additional bands of ASTER compared with Landsat provide an improved capability to discriminate, and potentially identify the surface vegetation and rock/soil composition. An overview of, and comparison between, the characteristics of ASTER, Landsat and other current satellite sensors were described by Michael (2012). In particular, the additional ASTER SWIR bands can detect the clay mineral absorption signature (e.g. sandstone in Figure 1) separately from carbonate absorption signature (e.g. limestone in Figure 1). ASTER's TIR bands can also discriminate quartz and silica-bearing rocks (e.g. sandstone, soil in Figure 1) by their absorption features in the 8–10 μm range. The ability of ASTER's VNIR, SWIR and TIR 14-band multispectral sensor to detect diagnostic absorption signatures of mineral (groups) is determined by its spectral resolution (i.e. bandwidth), specific wavelengths measured (Figure 1) and also its ground spatial resolution. These sensor characteristics determine its sensitivity to discriminate different surface components in order to uniquely identify mineral composition within a single digital measurement (e.g. pixel).

Mineral detection using ASTER

The use of ASTER satellite data products follows several decades of laboratory-based spectroscopy within the VNIR, SWIR and TIR wavelength regions for the measurement of minerals and mineral groups (Vincent & Thomson 1972; Hunt & Ashley 1979). In particular, the ferric oxide group (e.g. hematite and goethite), OH-bearing minerals (e.g. clays, micas, amphiboles) and other silicates have been shown to display diagnostic signatures within the VNIR, SWIR

and TIR wavelength regions, respectively (Sherman 1985; Clark et al. 1990; Grove et al. 1992; Salisbury & D'Aria 1992). Such spectral signatures exhibit absorption features whose depth in reflectance values (or emissivity within the TIR) can be approximately related to abundance or content of that mineral. Some mineral signatures (e.g. mica) also demonstrate shifts in the wavelength of their absorption reflectance minima (\sim 2200 nm) associated with compositional chemistry changes. Such inferred compositional changes of mica can be relevant for the interpretation of their possible metamorphic or alteration history (Duke 1994).

The effect of the ASTER sensor spectral resolution on its ability to detect and discriminate different minerals within common rock units and soils, can be demonstrated by re-sampling laboratory-measured mineral signatures into equivalent 14-band ASTER signatures (Hewson 2013). Overall, ASTER's VNIR and SWIR sensors show themselves capable of discriminating between broad mineral groups such as ferric iron oxide, AlOH and MgOH/carbonate. In addition, ASTER's five TIR bands are capable of discriminating varieties of quartz and broad silicate groups.

Past ASTER case studies

There have been several successful geological mapping case studies undertaken using ASTER since its launch in 1999. Studies within the semi-arid terrain of Mount Fitton in the northern Flinders Ranges of South Australia demonstrated the ability of ASTER to discriminate the minerals associated with the major

lithological units and also areas of hydrothermal alteration (Hewson et al. 2001). Rowan and Mars (2003) also showed that lithological mapping was feasible in areas of good exposure. Hewson et al. (2005), using Broken Hill NSW, data, successfully applied simply devised spectral indices (e.g. band ratios) using ASTER radiance imagery to map mineralogy. A more detailed explanation was offered in GS2013/1558 (Hewson 2013). This approach is the basis for many of the CSIRO and Geoscience Australian ASTER Geoscience Map Products (Cudahy 2012).

Some limitations to using the ASTER SWIR bands for mineral (group) mapping have been present in past case studies due to the crosstalk issue where stray light from band 4 'leaks' as an additive noise signal into bands 5 and 9 (Iwasaki et al. 2001). An algorithm and software were implemented to correct for this miscalibration issue (Iwasaki & Tonooka 2005). However, in areas of low ground reflectance (e.g. shadow, thick vegetation, dark surfaces), residual crosstalk effect is apparent and can lead to 'false anomalies' using spectral band indices (Hewson et al. 2005; Hewson & Cudahy 2011).

Early ASTER case studies also showed the usefulness of integrating processed ASTER map products with airborne geophysical data, such as radiometric (Hewson et al. 2003). In particular, sericite/mica can be discriminated within ASTER map products generated for the ALOH mineral group using potassium radiometric data at Broken Hill (Hewson et al. 2003). Integrating Landsat TM (Ricchetti 2000) and ASTER imagery (Hewson et al. 2006) with Digital Elevation Model (DEM) information has also improved the classification and interpretation of the geomorphology and geology. In particular, ASTER-interpreted quartz mineral occurrences related to transported sandy alluvial cover can be easily discriminated from silicified rock outcrops with slope and shaded DEM products (Hewson et al. 2006). Since the launch of the Australian CSIRO–GA Australian ASTER Geoscience Map products, Laukamp et al. (2013) recently demonstrated its application for mineral exploration in the Jervis Block arid environment of central Northern Territory. Further studies also showed their ability to map both lithological units and areas of hydrothermal alteration within the semi-arid Mount Fitton area of the northern Flinders Ranges (Hewson et al. 2013).

CSIRO–GA Australian ASTER geoscience map products

The Australian ASTER products released by CSIRO and GA provided the first continent-wide mosaic of satellite-derived mineral mapping (Cudahy 2012; Caccetta et al. 2013). Prior to the generation of such Australian continental scale compositional maps, isolated and independent industry and government agency projects provided useful, albeit sometimes haphazard, application of ASTER for limited Australian areas using variable methodologies and reference standards. The mosaicing of thousands of Australian ASTER radiance scenes were calibrated using many hyperspectral satellite reflectance reference surveys in conjunction with illumination and atmosphere-based gain and offset corrections (Cudahy 2012; Caccetta et al. 2013). This calibration of ASTER imagery using reflectance reference areas attempted to reduce the effects of crosstalk, variable illumination and ground cover conditions (Caccetta et al. 2013). Subsequent processing into band (ratio) parameters, targeting composition-related spectral absorption features, provided a generally reliable approach, for generating map products across Australia (Caccetta et al. 2013; Cudahy 2012). The values produced by these band parameter ratio products provided a unitless and relative estimate of abundance or indicator of composition depending on the nature of the described product. Masking of resulting band parameter products was performed to exclude areas of cloud cover, deep shadow, water bodies and significant vegetation followed by the application of consistent thresholds that best qualitatively to semi-quantitatively represented mineral (group) surface content and likely mineral species composition of rock/soil exposures. Table 1 summarises the 17 ASTER products and their inferred accuracies (Cudahy 2012).

NASA-developed World Wind software (<http://www.ga.gov.au/aster-viewer>) has been promoted as a user-friendly method of visualising these CSIRO–GA Australian ASTER geoscience map products in conjunction with topographic information and other geophysical datasets such as radiometric data. These ASTER map products in GeoTIFF file format can be accessed from the AuScope Discovery Portal (<http://portal.auscope.org/portal/gmap.html>) or CSIRO's site C3DMM (<http://c3dmm.csiro.au>). In this study, the ASTER map products in binary sequential (BSQ) format were also used to examine the effects of different histogram stretches and threshold values applied to a variety of band ratio imagery.

Table 1. Summary of the 17 CSIRO–GA compositional map products (Cudahy 2012).

Product name (product spatial resolution)	Surface composition / Example minerals targeted	Accuracy
1. False colour (30 m)	Standard VNIR product, green vegetation highlighted in red	N/A
2. Landsat TM Regolith Ratios (30 m)	Green vegetation versus different geological/regolith areas	N/A
3. Green vegetation content (30 m)	Green vegetation	Moderate
4. Ferric oxide content (30 m)	Hematite, goethite, jarosite	Moderate
5. Ferric oxide composition (30 m)	Hematite versus goethite	Moderate
6. Ferrous iron index (30 m)	As incorporated within silicates/carbonate	Moderate
7. Opaque index (30 m)	Includes carbon black (e.g. ash), magnetite, Mn oxides	Moderate
8. ALOH group content (30 m)	Phengite, muscovite, paragonite, illite, montmorillonite, kaolinite	Moderate
9. ALOH group composition (30 m)	Ordered kaolinite, Al-rich white mica (e.g. muscovite, paragonite) versus Al-poor (also Si- or K-rich) white mica (e.g. phengite)	Moderate
10. Kaolin group index (30 m)	Pyrophyllite, alunite, well ordered kaolinite	Moderate
11. FeOH group content (30 m)	Chlorite, epidote, jarosite, gibbsite, gypsum	Low
12. MgOH group content (30 m)	Calcite, dolomite, magnesite, chlorite, amphibole, talc	Moderate
13. MgOH group composition (30 m)	Dolomite, amphibole, chlorite versus calcite, amphibole	Moderate
14. Ferrous iron content in MgOH/carbonate (30 m)	Low ferrous iron carbonate / MgOH minerals (e.g. talc) versus High ferrous iron carbonate / MgOH minerals (e.g. chlorite)	Moderate
15. Silica index (90 m)	SiO ₂ content, quartz content enhanced by grain texture	Moderate
16. Quartz index (90 m)	Quartz	Low
17. Gypsum index (90 m)	Gypsum	Very low

Case study areas — environment and geology

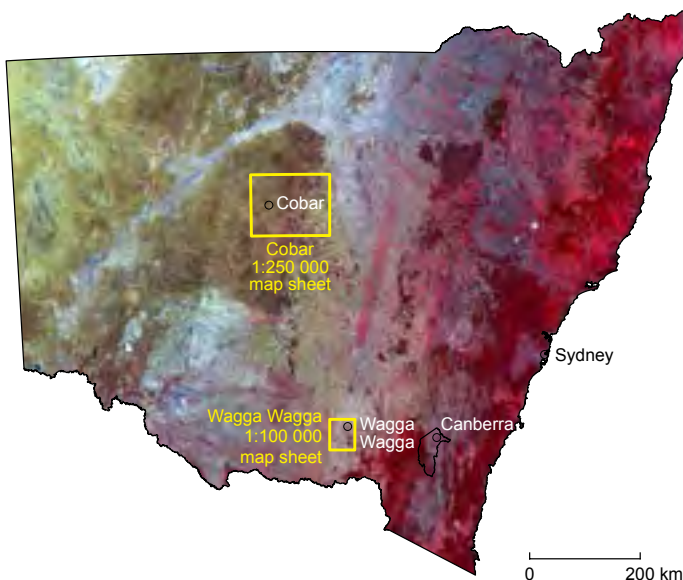


Figure 2. ASTER False colour map product for NSW, showing the 1:250K map sheet boundaries. The Cobar and Wagga Wagga study areas are outlined.

ASTER coverage of NSW

Mineral mapping across NSW has been extended by the CSIRO–GA ASTER map products for most of the state with its best mapping examples highlighted within the drier western half (Figure 2). The ASTER scenes were also best mosaiced seamlessly in the arid and semi-arid western half, where seasonal and yearly variations in vegetation are less significant — as shown by the ASTER False Colour (e.g. green vegetation shown in red). Figure 2 also shows the two study areas for this study, the Wagga Wagga 100K and the Cobar 250K map sheets.

WAGGA WAGGA 1:100 000 map sheet area

The area of the Wagga Wagga 1:100 000 map sheet of southeastern NSW was examined in this study and encompasses regolith and landforms typical of the Riverine Plains adjacent to the Murrumbidgee River (Figure 3). In particular, it has elevations ranging from 180 m to above 500 m, experiencing a moderate rainfall between 500 mm and 650 mm per annum (Chen 1997). The majority of the map sheet area is actively farmed, either as crops or under sheep or cattle grazing. Landforms consist of floodplains to moderately hilly areas with some eroded plateau exposures and piedmonts (Chen & McKane 1997). Chen (1997) described and analysed the geomorphology and landforms, in part using slope percent (%) estimates of the various floodplains and tributaries (1–2%), undulating plains and rises (3–5%), and hilly areas vulnerable to erosion (10–30%). Surface soils typically include clay-rich alluvial and gravels with a strong presence of aeolian (parna) sediments, particularly blanketing areas of lower relief. Extensively folded Ordovician metasediments, large intrusive Silurian granite bodies, and minor Devonian sandstones occupy hilly areas, mostly encompassing the eastern and southeastern parts of the Wagga Wagga 1:100 000 map sheet area (Raymond 1993).

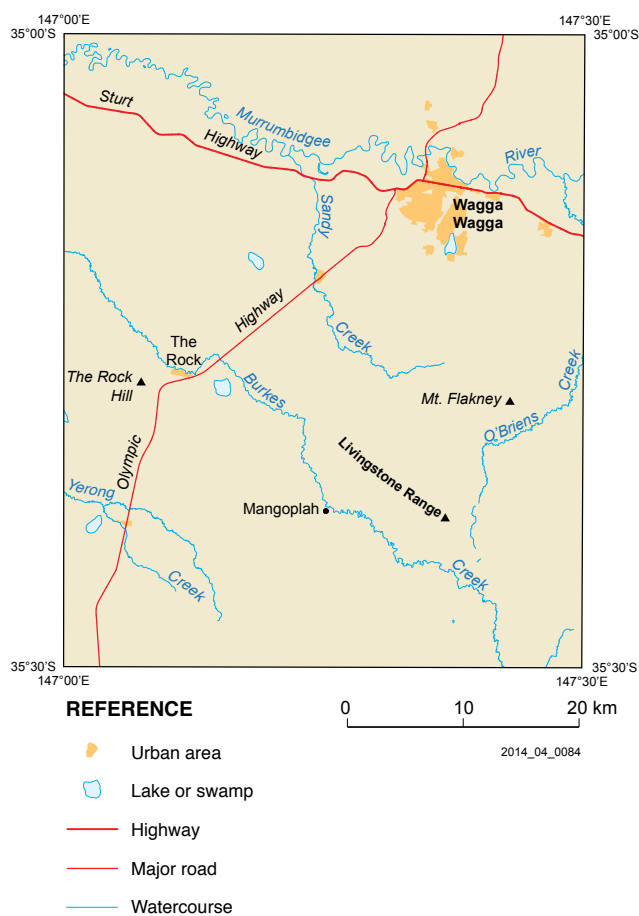


Figure 3. Location and selected watercourses within the Wagga Wagga 1:100 000 map sheet area.

The proximity of the Wagga study area to the Gilmore Fault, and the Gidginbung/Adelong gold deposits provided possible models and references in the search for prospective targets (Downes et al. 2004; Lewis & Downes 2008). The Adelong gold deposit is considered an orogenic gold orebody whilst the Gidginbung gold–copper deposit is regarded as a high-sulphidation epithermal type (Lewis & Downes 2008). Studies of the Lachlan orogenic gold deposits, including the Adelong deposit, generally show an alteration assemblage that includes sericite, muscovite–phengite and/or carbonates (Downes & Seccombe 2008), and are potentially mapped by the ASTER AIOH and MgOH/carbonate map products. The alteration at the Gidginbung deposit consists of several zones that include silica/quartz, kaolinite and illite (Downes et al. 2004) — also potentially mappable by the ASTER AIOH and Silica Index/quartz products. As a result, one of the main aims in this Wagga study area is to check the ability of the ASTER map products to discriminate such AIOH (e.g. sericite/white mica), MgOH/carbonate and silica/quartz content, associated with the Silurian granites and adjacent sedimentary/metasedimentary units. ASTER ferric oxide content and composition map products could also possibly assist with the interpretation of regolith landscape information.

COBAR 1:250 000 map sheet area

Cobar is in western NSW within a semi-arid environment (Figures 2, 4) and has an average annual rainfall of approximately 300+ mm (Chan et al. 2003). The area is characterised by predominantly erosional landforms, encompassing the catchment of the Macquarie and Bogan rivers with minor topographic relief and an average of 200–300 m above sea level (Chan et al. 2003). Contour intervals of 50 m, shown in Figure 4, highlight the mostly low relief penplain nature of the area's landforms. Agricultural cropping occurs in the eastern half of the Cobar 250K map sheet area and rangeland grazing is predominant within the western half.

The geological exposure of the various Palaeozoic metasedimentary and metavolcanic units of interest for economic gold and base metal deposits, are affected by a complex history of regolith development and transported alluvial/aeolian deposition (Chan et al. 2003; McQueen 2008). Weathering varies considerably but typically 20 m to 80 m thick (Chan et al. 2003). Palaeodrainage networks and palaeosurface landforms are also present amongst the current alluvial and colluvial landscape. Geochemistry exploration sampling and interpretation within this region requires a detailed knowledge and understanding of the nature and history of the regolith being sampled (Chan et al. 2003).

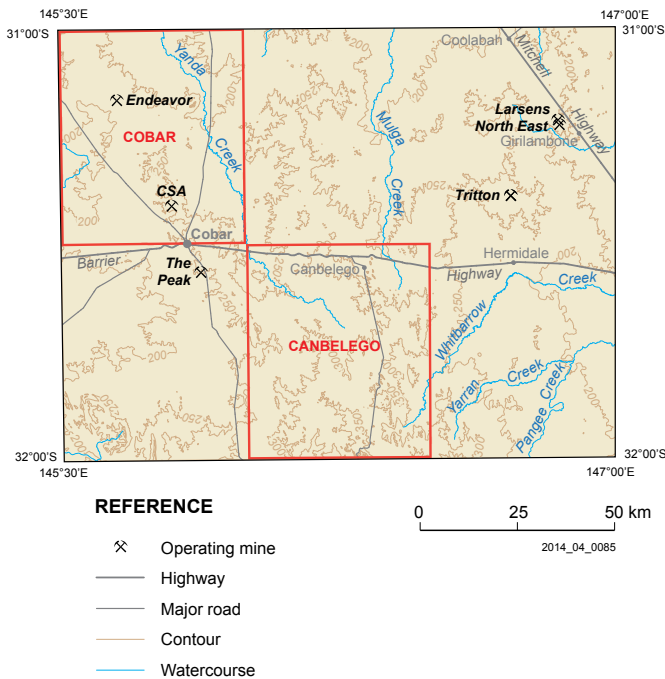


Figure 4. Cobar 250K map sheet area highlighting major mines, watercourses and 50 m elevation contour intervals. Topographic base data is from Geoscience Australia.

Shortwave Infrared (SWIR) spectroscopy of regolith samples has assisted an understanding of the boundary between transported and residual *in situ* material (Chan et al. 2003). In particular, information about clays (including kaolinite crystallinity) has been used to identify such boundaries (Cudahy 1997). Transported materials typically exhibit poorly crystalline or disordered kaolinite signatures while *in situ* outcrops show crystalline/well-ordered kaolinite signatures. The identification of the ferric iron oxide mineral hematite, versus goethite, can also be a useful indicator of the regolith history and nature of the surface exposure (Huntington et al. 1999). It is in this context that the recently released ASTER mineral map products, together with geophysical radiometric information, can potentially assist the interpretation of surface regolith landforms around Cobar, and also aid the analysis of geochemical surveys.

Datasets and methodologies

ASTER

GeoTIFF and BSQ binary format versions of the ASTER map products were both utilised in this study, as made available by CSIRO and GA via the GSNSW. The 17 ASTER products were visualised with ENVITM (<http://www.exelisvis.com>), ERMMapperTM (<http://geospatial.intergraph.com/Homepage.aspx>) and Global MapperTM (<http://www.bluemarblegeo.com/products/>

global-mapper.php) software, where map sheet boundaries, drainage and other relevant topographic Geographic Information System (GIS) shapefile information were incorporated. ERMMapperTM and Global MapperTM proved the most user friendly when integrating with geophysical and other datasets of different dimensions and origins. BSQ format versions of the ASTER map products were useful when examining variations of the imagery and generated mineral anomalies using different image histogram stretches and cutoff thresholds from those assumed in Cudahy (2012).

The ASTER acquisition dates of imagery used for the generation of mineral map products in the Wagga Wagga and Cobar study areas, were determined by examining the ASTER archive listed within the USGS Glovis site (https://lpdaac.usgs.gov/data_access/glovis). Data for the major portion of the Wagga Wagga 100K map sheet area were acquired with ASTER on 11/1/2001. The geologically relevant western half of the Cobar 250K map sheet area, with minimal cropping and cultivation (inc. Cobar 100K, Canbelego 100K map sheet areas), was acquired by ASTER on 19/9/2003.

Airborne geophysics

Various radiometric and filtered aeromagnetic or Total Magnetic Intensity (TMI) ERMMapper and GeoTIFF files, processed into 50 m grids, were obtained by the GSNSW for the Wagga Wagga 100K map sheet area. High-frequency filtered TMI data such as tilt-angle filtered and first (1VD), second (2VD) vertical and horizontal (1HD) derivative files were also examined for near-surface magnetic anomalies relevant for comparison with the radiometric and ASTER data. TMI imagery was also processed as Reduced to the Pole (RTP) TMI versions to adjust for Earth's magnetic declination etc. Radioelements potassium (K), thorium (Th) and uranium (U), and the ternary RGB composite imagery (e.g. Red K, Green Th, Blue U) were useful to compare with surface remote sensing compositional imagery although typically that senses deeper into the subsurface (to ~30 cm). Airborne radiometric data, processed as 100 m grids were also used for the Cobar 250K map sheet study. ERMMapperTM, and to a lesser extent ENVI™, were used for examining and image processing the airborne geophysical datasets.

Digital elevation models (DEMs)

DEMs were available from the GSNSW airborne geophysics radar altimeter (at 50 m grid cells), the ASTER GDEM Version 2 (<http://asterweb.jpl.nasa.gov/gdem.asp>) at 30 m (x, y) spatial resolution and the Shuttle Radar Topography Mission (SRTM) at

80 m (x, y) spatial resolution (<http://www2.jpl.nasa.gov/srtm/>). Higher resolution SRTM DEMs at 30 m (x, y) were also accessible via the NSWGS for this particular government study although were found to be somewhat noisy within the Wagga Wagga and Cobar areas. ENVI™ was used to process DEM data into topographic models that included slope% and artificial sun-shaded relief imagery. The SRTM DEM information was found to generate the best slope product. Figure 5a displays the SRTM 80 m slope for relief greater than 10% combined with landscapes of Chen (1997), highlighting that these steeper slopes occur within divisions IV and V.

Auscover fractional landcover

Australia's land surface has been recently analysed for fractional cover percentages of bare ground (e.g. soil, rock outcrop), green vegetation and dry vegetation cover as part of the Terrestrial Ecosystem Research Network (TERN; <http://www.tern.org.au/>). Datasets are available as part of this project via the AusCover data facility (<http://data.auscover.org.au/>). Several

different versions of fractional cover information based on different algorithms and satellite sensors have been generated, and are currently in the process of validation across Australia. In this study, the satellite Landsat TM 5- and 7-based fractional cover analysis provided high 30 m spatial resolution for the Wagga Wagga and Cobar study areas. This coverage information was generated by algorithms described by Scarth et al. (2010) and available via AusCover as binary NetCDF data tiles (<http://data.auscover.org.au/xwiki/bin/view/Product+pages/Landsat+Fractional+Cover#HLinktothedata>). The Landsat fractional cover estimates were generated from imagery recorded within a few days of both the Wagga Wagga and Cobar ASTER image acquisition dates listed above. Figure 5b displays the fractional cover product as a RGB composite for bare ground, green and dry vegetation for the Wagga 100K map sheet area generated from Landsat 7 acquired on 10/1/2001. In this study, several masks based on the fractional cover layers were devised and applied on the ASTER maps. However, the photosynthetic vegetation fraction for values less than 45% were used to refine (i.e. filter) the final ASTER map examples.

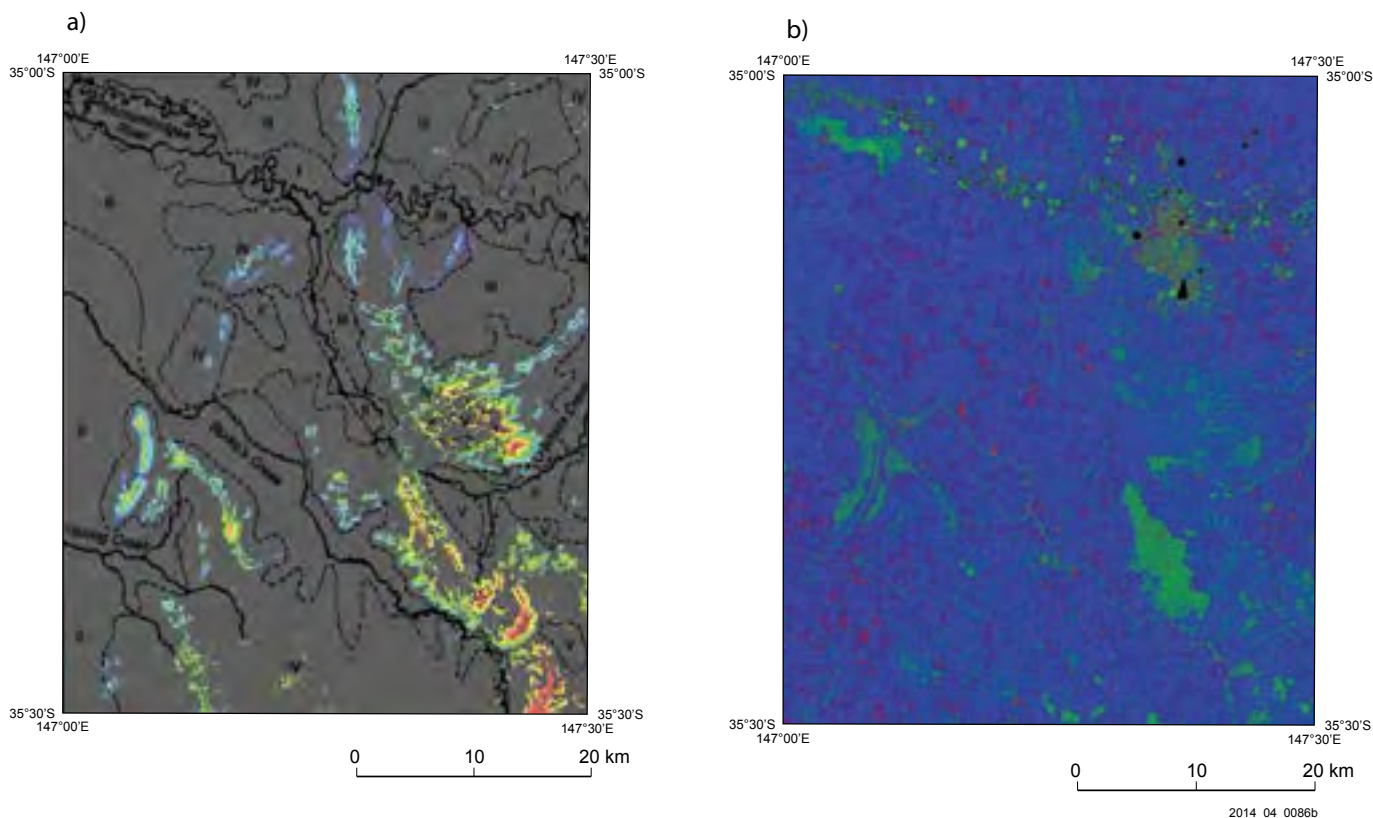


Figure 5. a) Wagga Wagga 100K landscape divisions overlying SRTM 80 m DEM slope greater than 10%, Blue: 150 to Red: 300m. Landscape divisions: (I) Murrumbidgee floodplains; (II) alluvial plains of local streams; (III) undulating plains, rises, and long footslopes; (IV) hilly areas; and (V) eroded plateau and piedmont plains (Chen 1997); b) Wagga 100K Landsat 7-derived fractional cover RGB image. Red: bare ground, Green: photosynthetic vegetation, Blue: non-photosynthetic vegetation; (linear stretch, 0–100%).

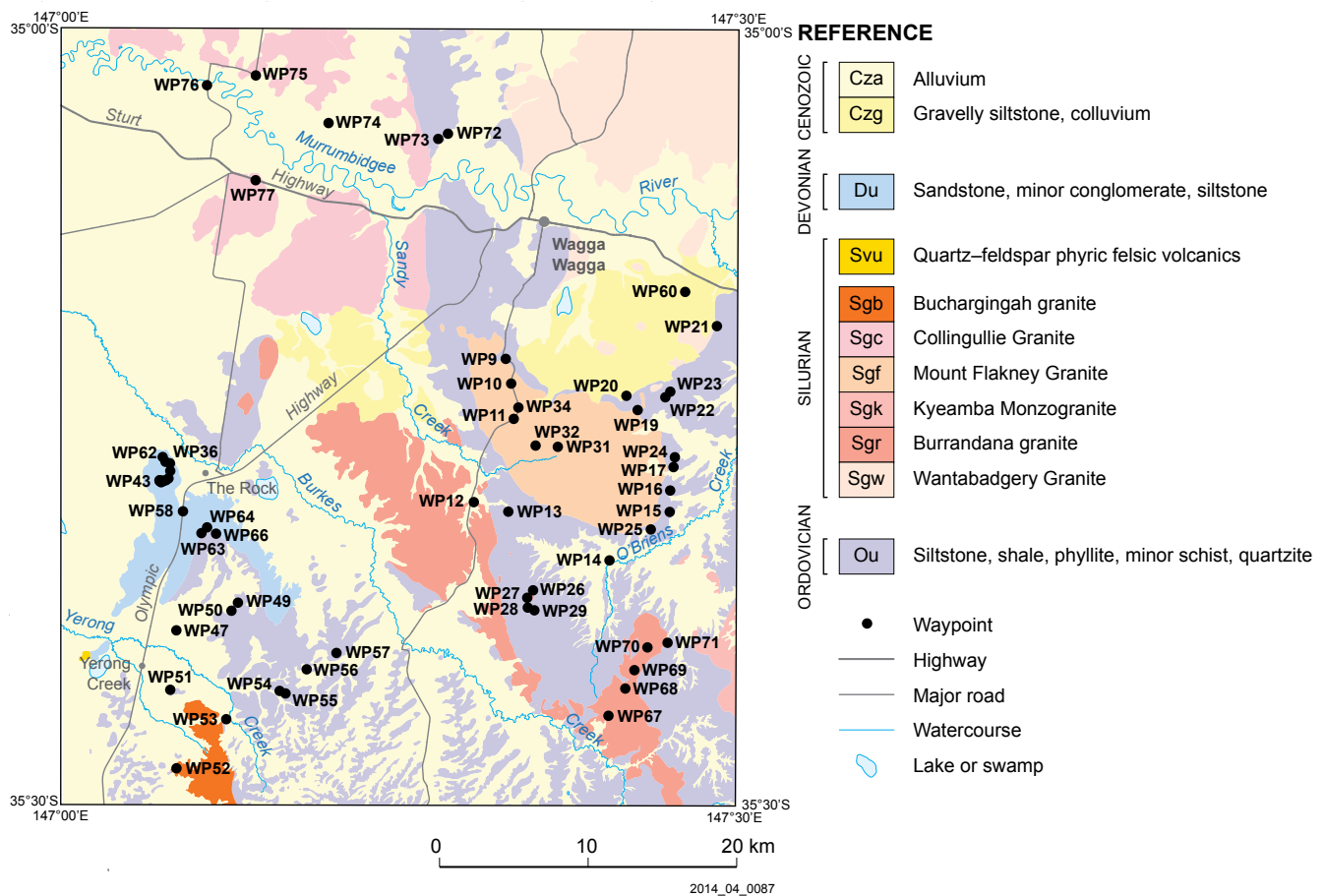


Figure 6. Wagga Wagga 100K geological map (Raymond 1993) and the observed field localities (WP).

Data integration strategies

Past integrated studies of spectral, airborne geophysics and DEM data have shown the usefulness of simple RGB composite imagery such as ASTER-derived AIOH content with radiometric K, draped over high-pass filtered magnetic data (Hewson et al. 2003). Comparing ASTER products with slopes modelled from DEMs was found particularly useful for discriminating mineral occurrences associated with transported alluvium versus outcrop (Hewson et al. 2006). In this study, slope percent imagery derived from the Wagga Wagga 100K SRTM DEM data was processed with a threshold to extract ('mask') only areas greater than 10% in order to focus on potentially hilly and piedmont rock/talus outcrop exposures within the combined ASTER-geophysics products. Shaded relief imagery of the DEM was also used with ERMMapper™ as an 'Intensity' base layer to RGB composite imagery of ASTER and geophysics data products. Shaded relief DEM imagery for the Wagga Wagga study area was generated assuming a sun elevation of 60° and azimuth of 072° to simulate the illumination conditions when the relevant ASTER imagery was acquired on 11/1/2001 at 10.30am.

Field studies and sample spectroscopy

Field sampling and validation of identified ASTER mineral map anomalies were undertaken in the Wagga Wagga area during April 2013 in the form of observed waypoints and as sampling localities. A total of 69 localities were visited ('WPxx', Figure 6), of which 29 were sampled for rocks and soils. Full descriptions of field waypoints, sample localities and associated geological/landform information are included within the GS2013/1558 DVD database (Hewson 2013). All collected field samples were measured with the Analytical Spectral Device Inc. (ASD) Terraspec 4 VNIR-SWIR spectrometer (<http://www.asdi.com/products/terraspec/terraspec-hi-res-mineral-spectrometer>). At this stage no validation or field sampling has been undertaken within the Cobar 250K map sheet area.

ASTER validation study

Several localities within the Wagga Wagga 100K map sheet area were used for validation or 'ground truth' sites for the ASTER map products. The Wagga Wagga Airport and RAAF base provided useful dark ground targets to test for possible crosstalk issues (Figure 7a). The ASTER False Colour (Figure 7b) map product showed these dark or low-albedo surfaces. Residual crosstalk effect is a possible explanation for the corresponding AIOH group content anomalies (red and green areas, Figure 7c). Multiple spectral reflectance measurements were undertaken at each site with the TerraSpec 4 ('ASD') spectrometer using its hand-held probe. These measurements were averaged and resampled to ASTER spectral resolution to ascertain any possible AIOH-like SWIR signature (Figures 8a, b). Tarmac at the Wagga Wagga Airport and the RAAF base exhibited low overall reflectance and an absence of any effective average ASTER AIOH spectral absorption signature centred at band 6 (2200 nm) (Figure 8a, b).

Additional validation sites were also studied to examine ASTER's geological/mineral mapping invariant targets with minimal vegetation. In particular, gravel pits within the Wagga Wagga 100K map sheet area were identified for sampling and ASD Terraspec measurements. Waypoint WP52 (Sample WG21 site) within a granite gravel pit of approximately 100 m x 150 m was located on site (Figure 9 a–c) and within the 2001 ASTER map products (Figure 10a–c). The corresponding ASTER map products for the WP52/WG21 site showed reasonable spatially coherent anomalies for the ASTER AIOH, Silica Index and to a lesser extent, the Ferric Oxide anomalies. A four ASTER pixel subset within this gravel pit gave AIOH group content and ferric iron content values of 2.27 and 1.4, respectively. ASD derived equivalent ASTER AIOH group content and ferric iron content ratio products gave favourably comparable values of 2.42 and 1.47, respectively. Within the same gravel pit subset area, the Landsat derived fractional photosynthetic (e.g. green veg.) cover product also showed a low cover value of 23% (Figure 10d).



Figure 7. a) Google Earth image of ASTER validation sites at Wagga Wagga Airport (GP5), waypoints WP59, WP60 and RAAF parade ground (GP6), waypoint WP61; b) ASTER False colour image c) ASTER AIOH group content (purple/blue: low to red: high content).

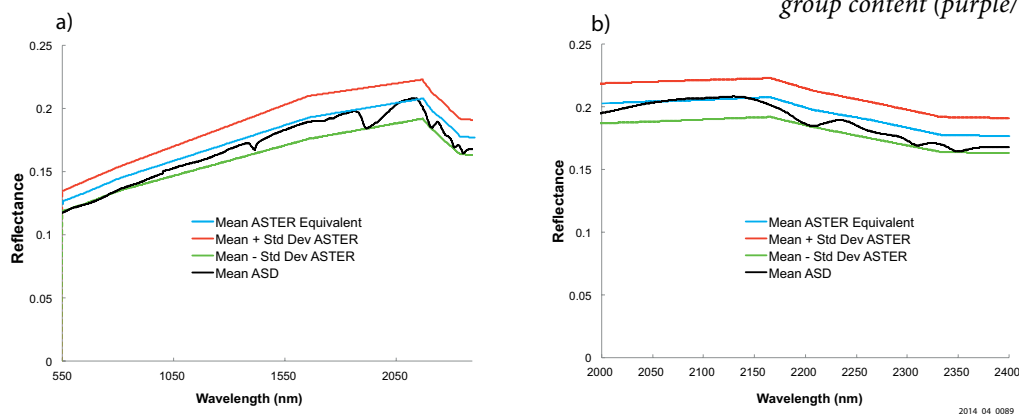


Figure 8. Wagga Wagga Airport tarmac (WP59–60): ASD and resampled ASTER equivalent signature (mean \pm standard deviation) for a) the VNIR–SWIR wavelengths and b) close up for SWIR wavelengths.

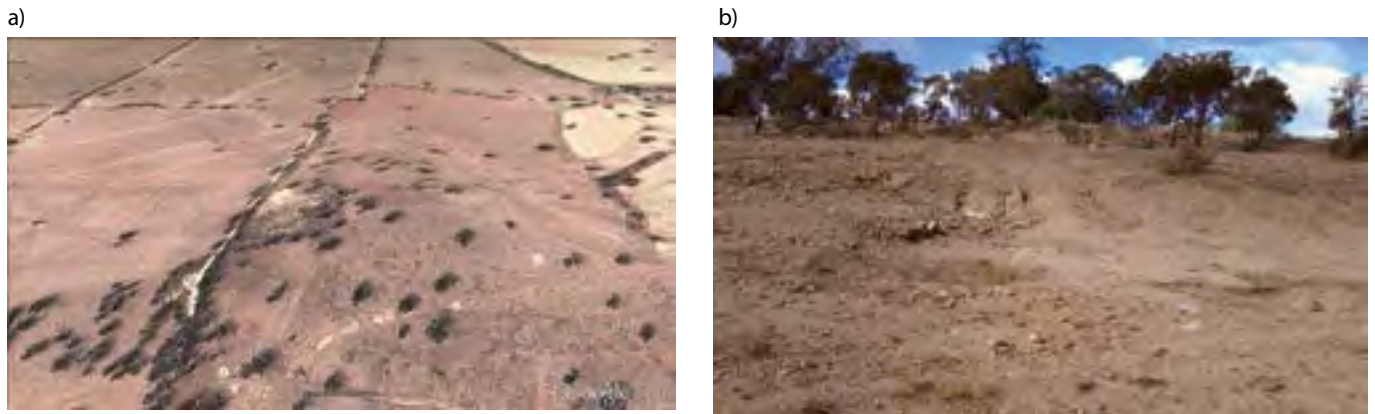


Figure 9. a) Google Earth image of ASTER geological validation site, WP52/WG21; b) Granitic gravel pit at WP52/WG21; c) ASD Terraspec spectral signatures of granite/gravel showing ferric iron and pronounced AIOH diagnostic spectral features at 880 nm to 1000 nm, and 2208 nm, respectively. Equivalent ASTER resampled signatures (asterisks) show detectable features, particularly for the AIOH SWIR feature.

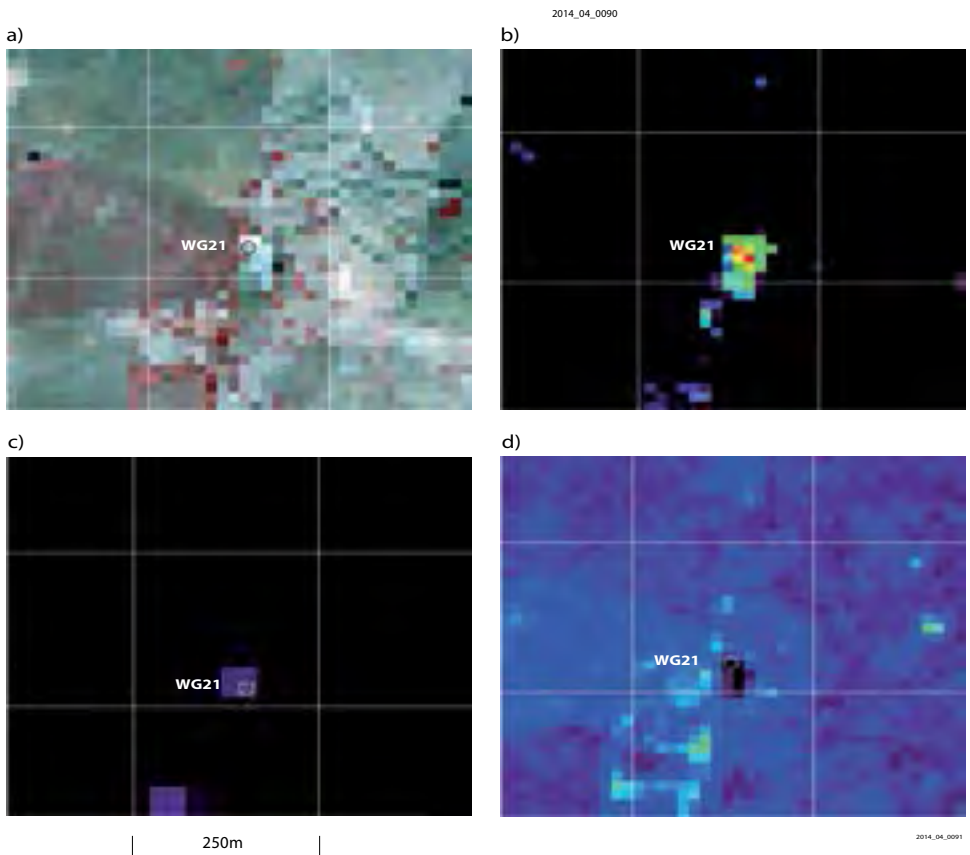
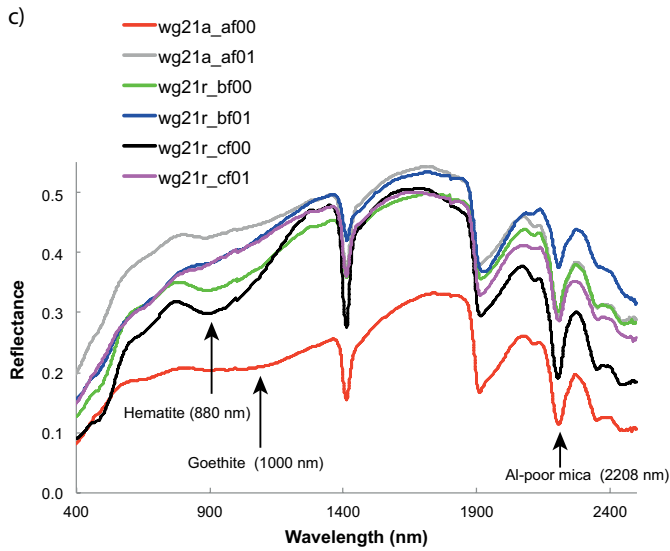


Figure 10. a) ASTER False Colour image of WP52 granitic gravel pit; b) ASTER AIOH group content; c) ASTER Silica Index; d) Landsat fractional cover - photosynthetic cover. Images b-d display map product values from low (purple/blue) to high (red) values. Grid cell is 250 m square.

Results

WAGGA WAGGA 1:100 000 map sheet area

ASTER map products

The Australian ASTER GeoTIFF map products were initially examined individually for the Wagga Wagga 100K map sheet area. Several of the 17 products did not show significant anomalies related to geological features and were limited to (cultivated) cropping patterns at best. In particular, the ASTER imagery used here was acquired in mid-summer 2001 and highlighted exposed fallow fields and soils (Figure 11). The ASTER False Colour map product (Figure 11) also highlighted the town of Wagga Wagga and several vegetated areas with topographic relief (dark red to dark grey). A slight boundary anomaly is apparent at the extreme northwestern edge of the 100K scene from a change of ASTER image scenes.

ASTER's green vegetation content product (Figure 12a) corresponds approximately with areas of red shown in the ASTER false colour product (Figure 11) although this green vegetation content product is more correctly generated by a band ratio (bands 3/band 2), targeting the chlorophyll 'red edge'. Exposed soil and fallow crop fields have no or low green vegetation anomalies (blue) on the floodplains and lowlands while vegetation is highlighted

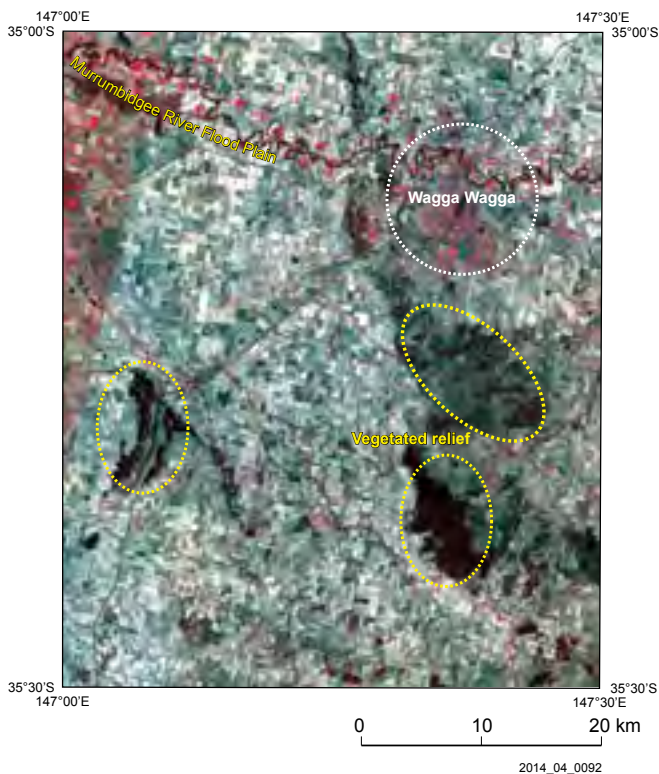


Figure 11. ASTER false colour products within Wagga Wagga 100K map sheet area.

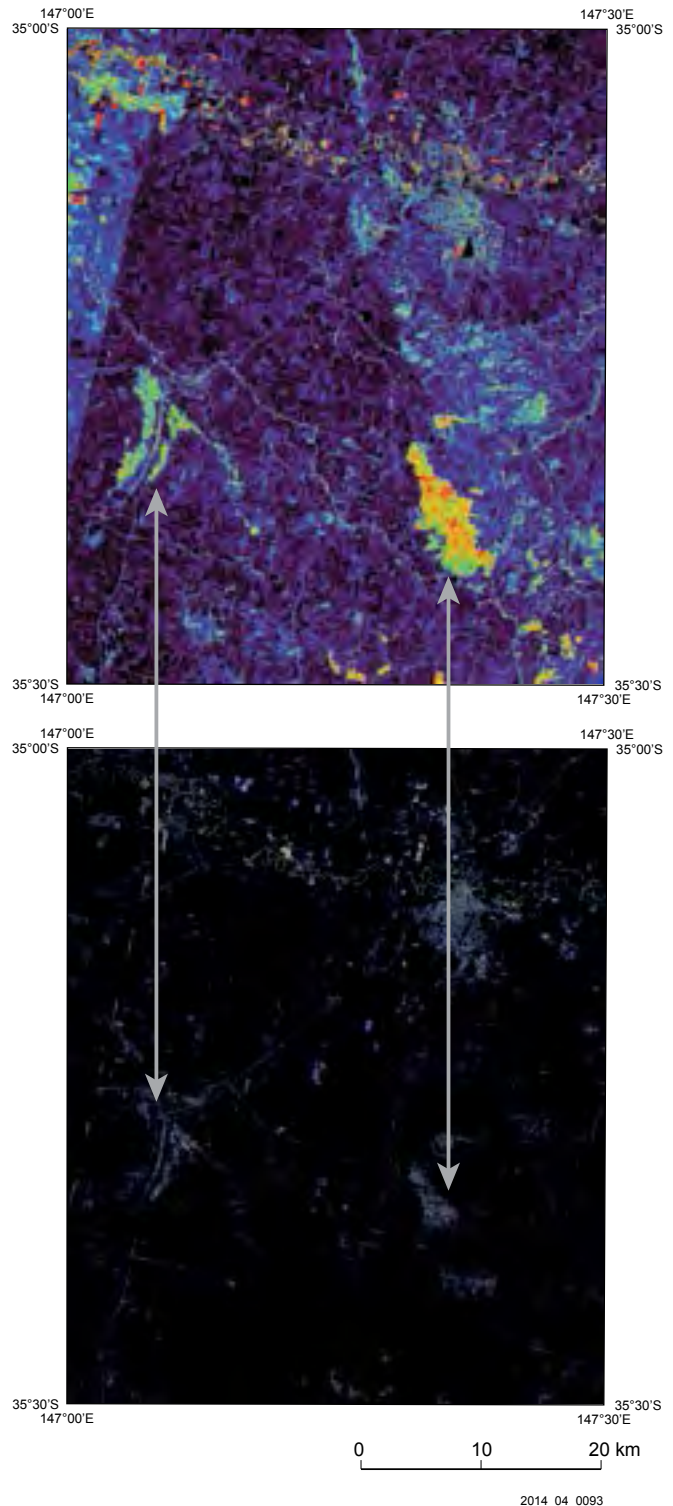


Figure 12. a) Wagga Wagga 100K ASTER green vegetation product (blue: low; red: high content); b) ASTER AIOH content (blue: low; red: high content).

within areas of topographic relief (Figures 11, 12a). ASTER's AIOH content product (Figure 12b) shows very limited clay anomalies except for the Wagga Wagga township and an apparent association with vegetated occurrences shown in the green vegetation product (Figure 12a). A green vegetation mask, based on the ASTER product, was applied during the generation of the AIOH composition map product and minimal anomalies were apparent.

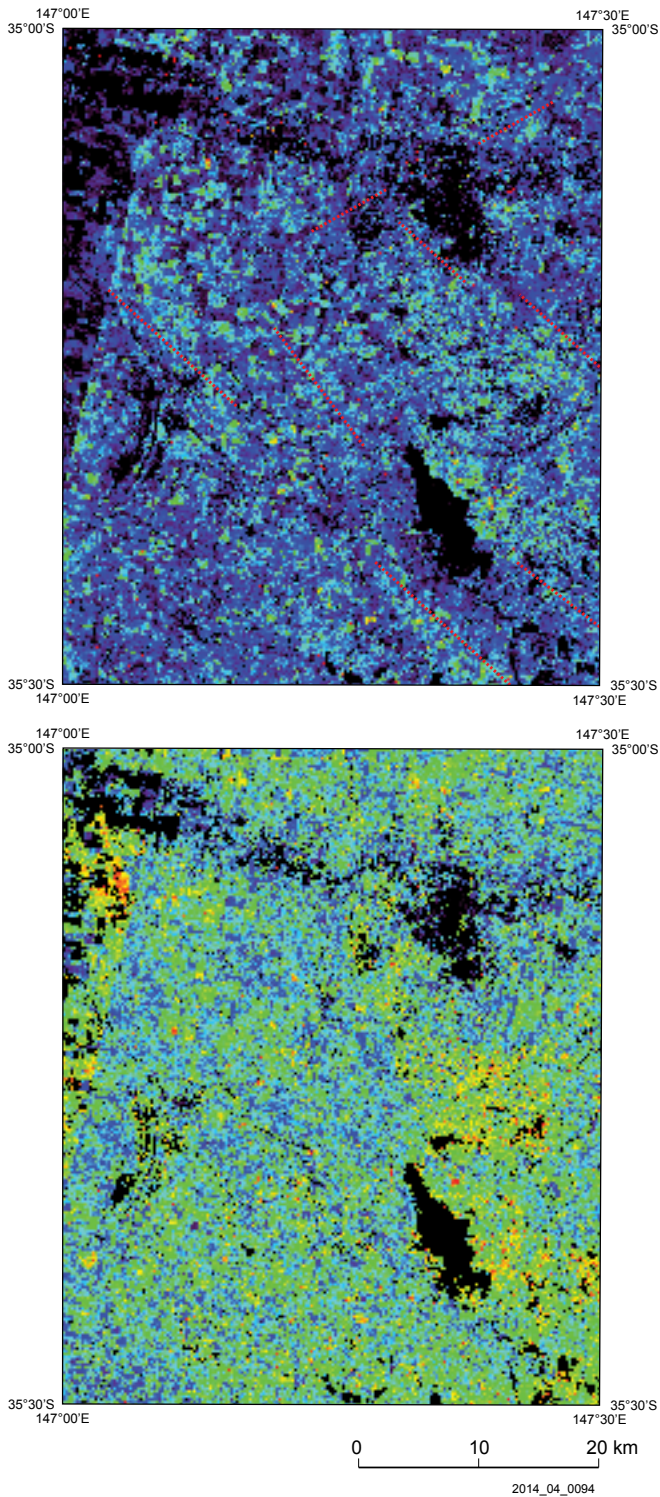


Figure 13. a) Wagga Wagga 100K ASTER ferric oxide content (blue: low; red: high); and b) composition map products. Apparent trends in the ferric oxide content are shown in red dashed lines.

ASTER's ferric oxide content and composition products (Figures 13a, b) show elevated values in contrast with the ALOH group content product (Figure 12b). There is also some variation in composition from the interpreted goethite-rich (blue–cyan) to hematite-rich (red–yellow) (Figure 13b). Some linear trends were apparent although the anomalies were often biased by the cropping patterns and exposed paddock soils. Nonetheless some linear trends (red dashed lines in

Figure 13a) show boundaries and possible lineaments related to floodplain alluvium, regolith or geological units. Although Cudahy (2012) described the ferric oxide content as having moderate accuracy, a comment is also noted for the potential of pixel spectral mixing errors and an inverse relationship with the green vegetation product. This could also be either related to the obscuring effect of vegetation/crops, or spectral signature ambiguities given the proximity of VNIR spectral features. The ASTER FeOH and ferrous iron products in the Wagga Wagga 100K map sheet area did not generate coherent or distinct features apart from some isolated paddock anomalies.

The ASTER MgOH group content and composition products showed minimal occurrences except for some anomalies in the far southwestern corner which occupied farm fields adjacent to Ordovician metasedimentary rocks. Likewise the kaolinite group Index showed only minor anomalies. Both the ASTER MgOH group content and composition and kaolinite index products were masked for green vegetation during processing (Cudahy 2012). The Silica Index (Figure 14) proved to have less noise and highlighted more anomalies than the ASTER quartz index, although the range in values and image contrast were limited. Subtle anomalies highlighted by the Silica Index generally occurred within paddocks corresponding to low green vegetation, and also as broader subtle variations (Figure 14).

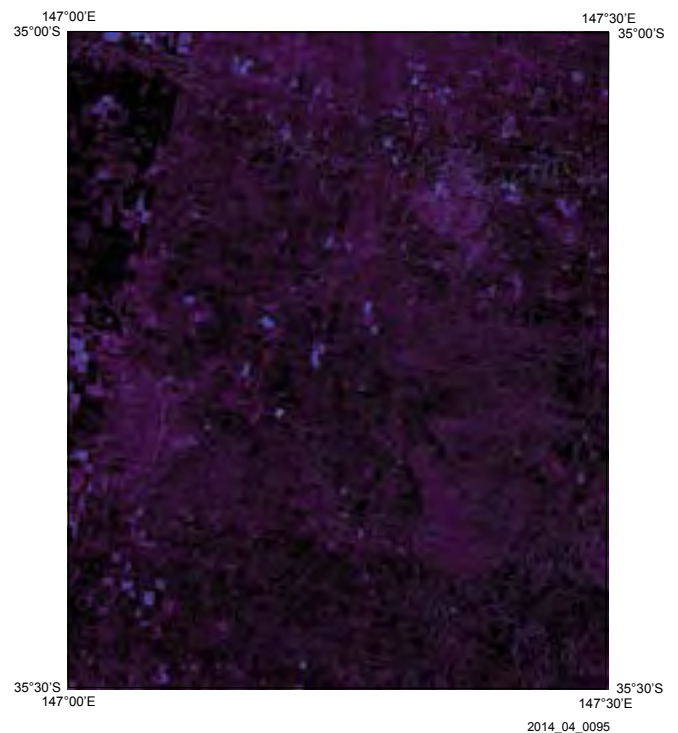


Figure 14. Wagga Wagga 100K map sheet area ASTER silica index.

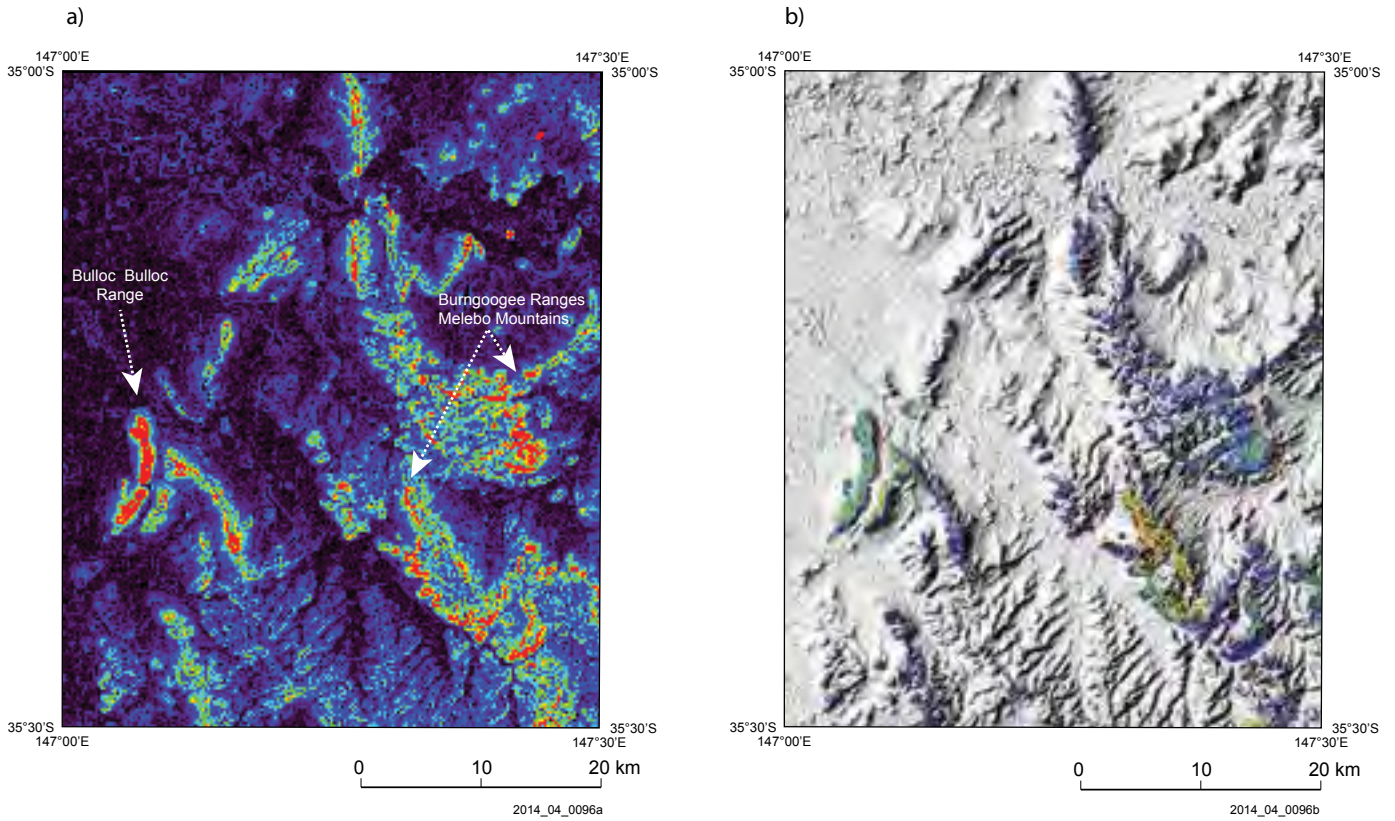


Figure 15. a) Wagga Wagga 100K SRTM 80 m slope% (blue: low; red: high); b) SRTM 80 m sun-shaded imagery draped with ASTER green vegetation product (Figure 12a) masked for slope >10%.

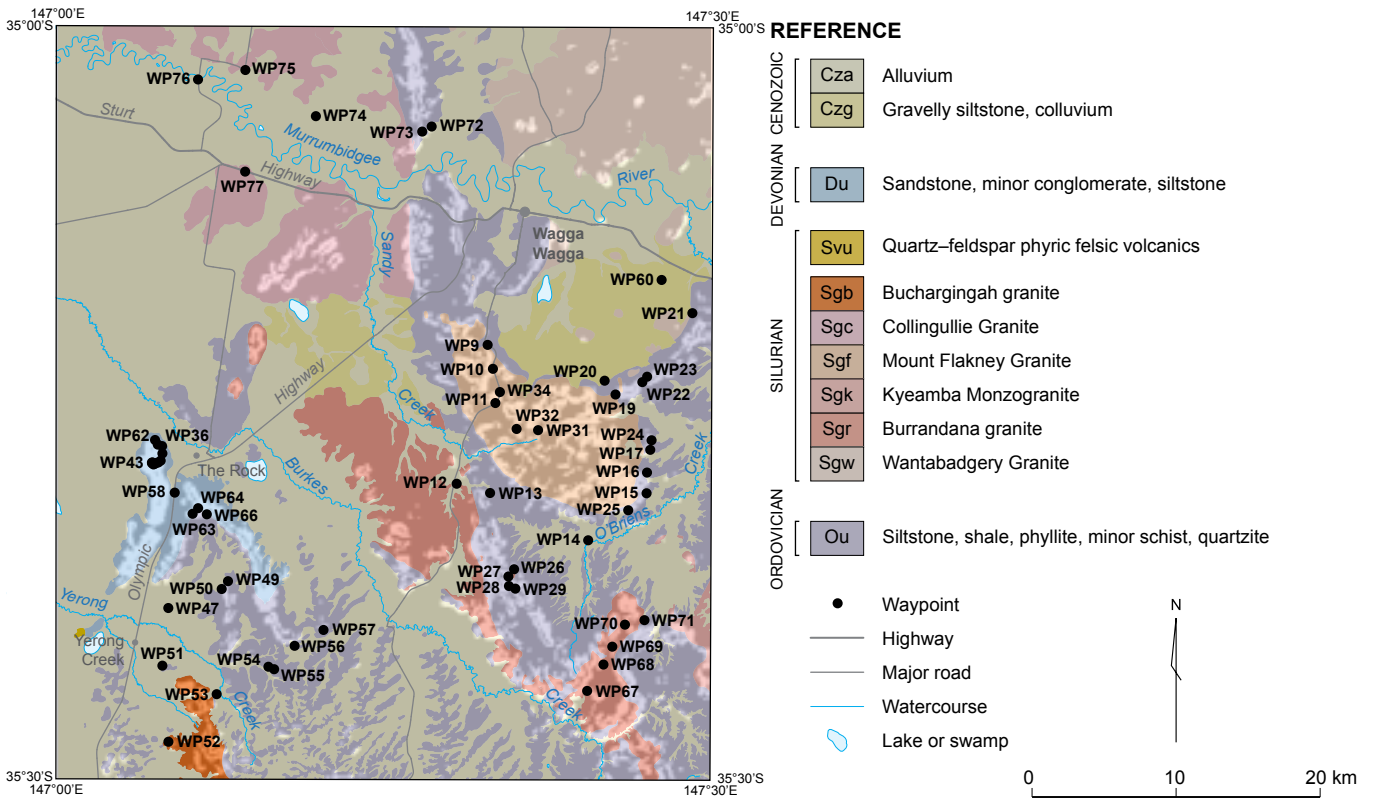


Figure 16. Wagga Wagga 100K geology map (Raymond 1993) combined with SRTM 80 m slope >10% showing geological units within areas of high relief.

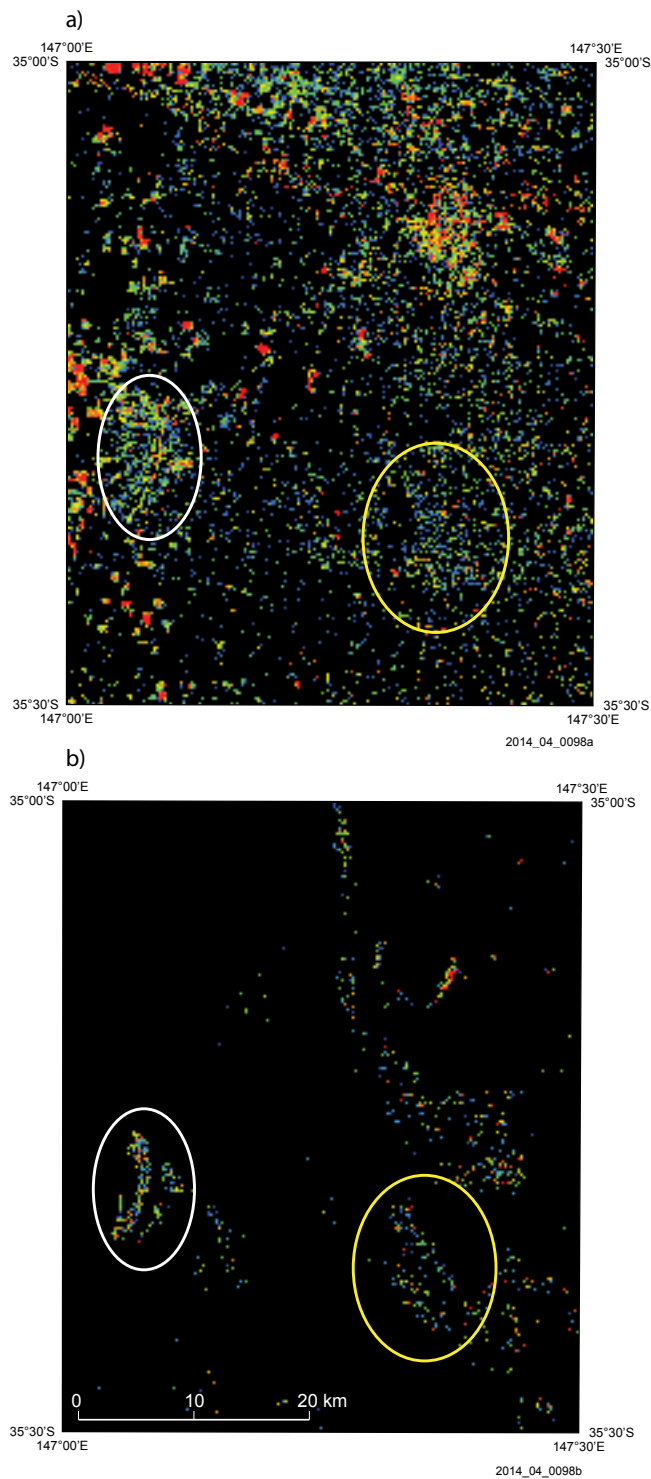


Figure 17. a) Wagga Wagga 100K ASTER Silica Index product generated with a histogram equalisation stretch; b) Histogram equalised ASTER silica index masked for slope >10%. (purple/blue: low to red: high content). Areas highlighted are Bullock Bullock Range (white) and Livingstone National Park (yellow).

The nature of the geomorphology and extensive agricultural cultivation of the Wagga Wagga 100K sheet area prompted the use of DEM data to discriminate the likely geologically exposed areas. Processing the SRTM 80 m DEM for slope% information highlighted the major ranges and topographic relief (Figure 15a). Sun-shaded DEM imagery also highlighted these landforms (Figure 15b). Generation of a mask based on slopes greater than 10% was useful to observe relationships with the various ASTER products. For example, when ASTER's green vegetation product, masked within areas of slope >10% is combined with sun-shaded imagery, much of the higher relief is observed to be moderately to highly vegetated (Figure 15b). Figure 16 shows simplified geological units combined with SRTM data.

An attempt to overcome the limited range of anomalies observed within the Wagga Wagga 100K ASTER silica index product (Figure 14) using a histogram equalisation stretch, within the same data range, highlighted both more noise and some coherent anomalies (Figure 17a). Masking of this product with SRTM Slope% product greater than 10% (Figure 17b) helped to discriminate exposed geological units as shown in Figure 16. Elevated areas of the quartz-rich sandstone of Bullock Bullock Range and metasedimentary rock of Livingstone National Park were highlighted by this approach (Figure 17b).

Geophysical products

A similar approach to displaying and enhancing the Wagga Wagga 100K ASTER map products was applied to the airborne radiometric data where anomalous regions were extracted within the areas of elevated slope. Histogram equalisation stretching of the K, Th and U radioelements highlighted a mixture of alluvial deposition and outcropping geology (Figure 18a). The potassium data coherently mapped the alluvium and floodplains of Burkes Creek and the Murrumbidgee River (Figure 18a). The Mount Flakney Granite and the Bullock Bullock Range Ordovician (Ou) and Devonian sandstones (Du) were highlighted as anomalous using the entire 100K map sheet dataset (with histogram equalisation) but more subtle variations in radioelement composition were apparent when slope masking was applied and a simple 2% linear histogram was applied for image stretching (Figure 18b). Compositional variations within these units appeared to be enhanced by limiting the focus to areas of higher relief. Increased thicknesses of aeolian deposits, alluvium or colluvium on lowlands and areas of reduced slope may mask and dilute radiometric sensing of some of these units.

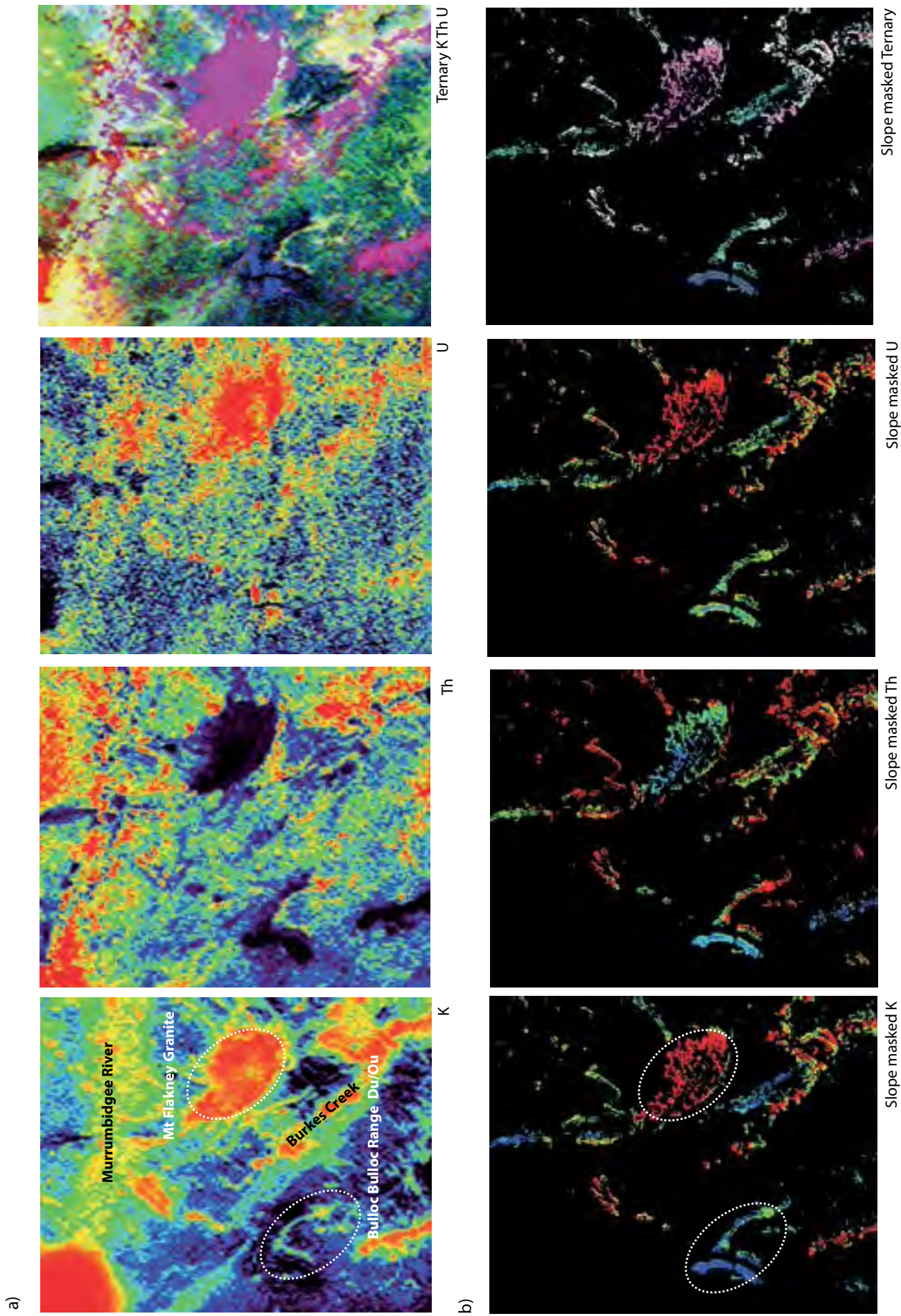


Figure 18. a) Wagga Wagga 100K airborne radiometric data, K, Th, U and as a Ternary image (RGB: K, Th, U), displayed with a histogram equalisation stretch; b) K, Th, U Ternary image masked for slopes >10%, displayed with a 2% linear histogram stretch. Geological features discussed in text are circled.

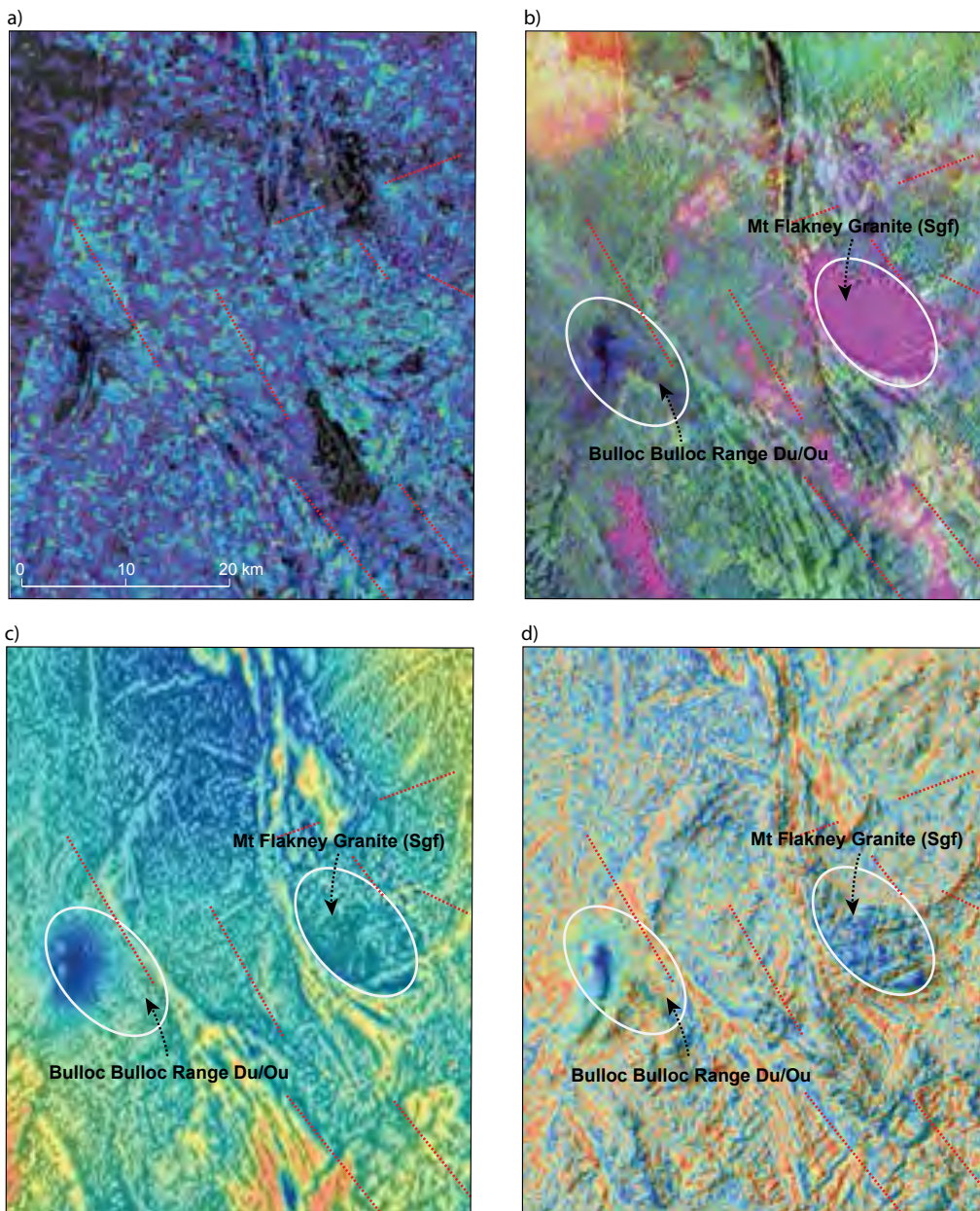
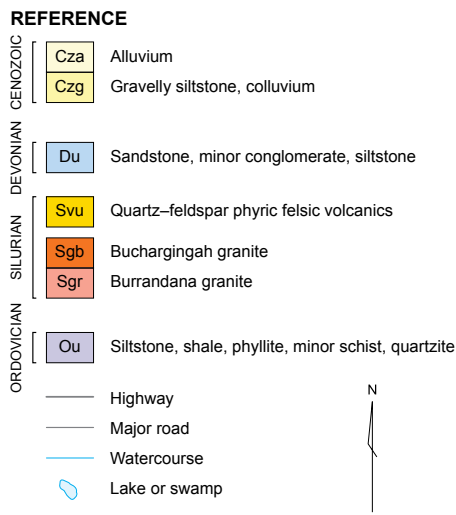
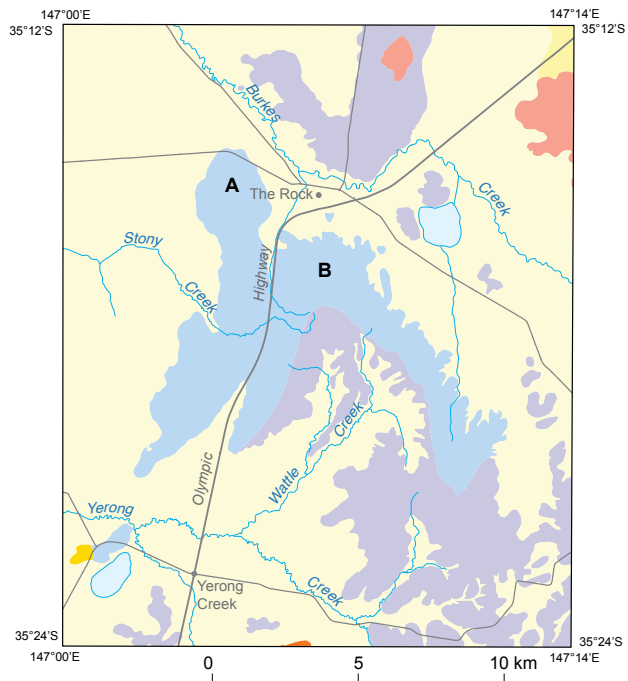


Figure 19. Apparent trends in the ASTER ferric oxide content (from Figure 13a) are shown as red dashed lines. a) TMI 1VD (greyscale) overlain with ASTER ferric oxide content. b) TMI 1VD (greyscale) overlain with K, Th, U Ternary RGB imagery (Red: K, Green: Th, Blue: U). c) RTP TMI (greyscale) over tilt-filtered RTP TMI (pseudocolour), d) Sun-shaded SRTM DEM (greyscale) overlain with tilt-filtered TMI (pseudocolour).

2014_04_0100

Filtered aeromagnetic data for the Wagga Wagga 100K map sheet area were used in an effort to extract structural information and also to highlight near-surface trends of iron-bearing units/magnetite and possible correlations with the ASTER map products. ASTER's ferric oxide content showed some trends, albeit revealed within exposed paddocks (Figure 13a), that showed northwest-trending and some possible northeast-trending features that correlated approximately with First Vertical Derivative (1VD) TMI lineaments (Figure 19a). The VNIR spectral signature of magnetite is essentially aspectral and not likely to be revealed by the ASTER Ferric Oxide Content product directly. However, weathering of magnetite-bearing rocks may possibly be associated with increased ferric iron oxide minerals within soils exposed here. Integrating radiometric ternary imagery over TMI 1VD (Figure 19b) reveals similar northwest trends as Figure 19a. In addition, Figure 19b reveals a

complex series of north-northwest-trending lineaments along the western boundary of the K-rich Mount Flakney Granite and northwest-trending lineaments east of the sheared Bulloc Bulloc Range Devonian and Ordovician units. RTP TMI over tilt-filtered Reduced to the Pole (RTP) TMI (Figure 19c) highlighted several lineaments with some corresponding to those interpreted with ASTER ferric oxide and radiometric data (Figure 19a, b). The integration of tilt-filtered TMI over sun-shaded SRTM DEM (Figure 19d) also revealed some correlation of north-northwest and cross-cutting north-northeast lineaments with topographic relief and valleys (Figure 5a) related to either outcropping geological units or possible structural and tectonic movements. The tilt-filtered TMI within this Wagga 100K area appears to reveal increased high-frequency features and anomalies useful for detailed interpretation.



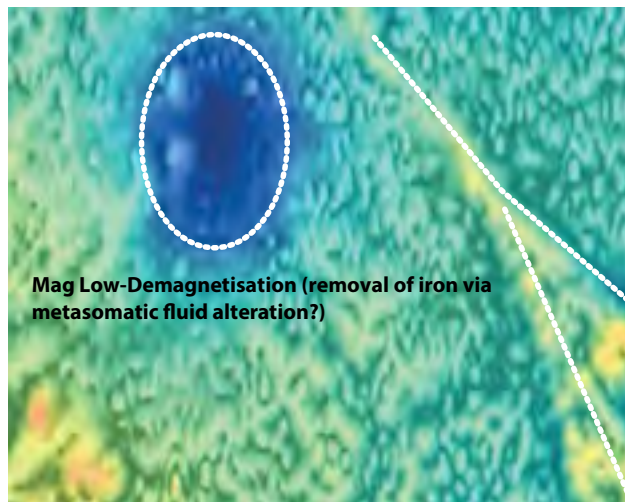
2014_04_0101

Figure 20. Location of The Rock Hill (A) and Flowerpot Hill (B) on part of the Wagga Wagga 100K geological map (Raymond 1993).

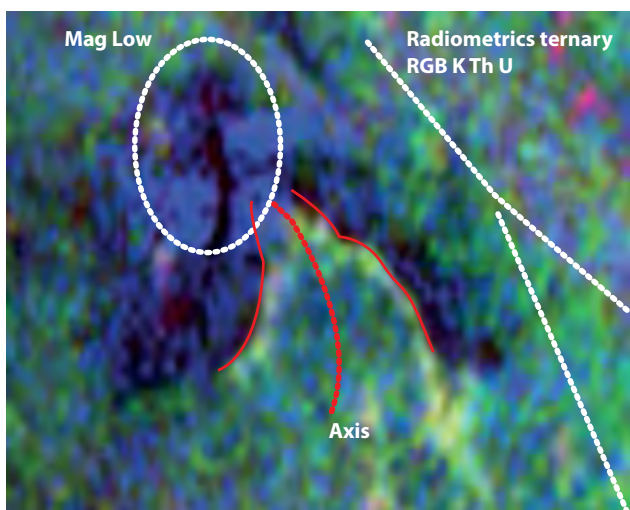
a)



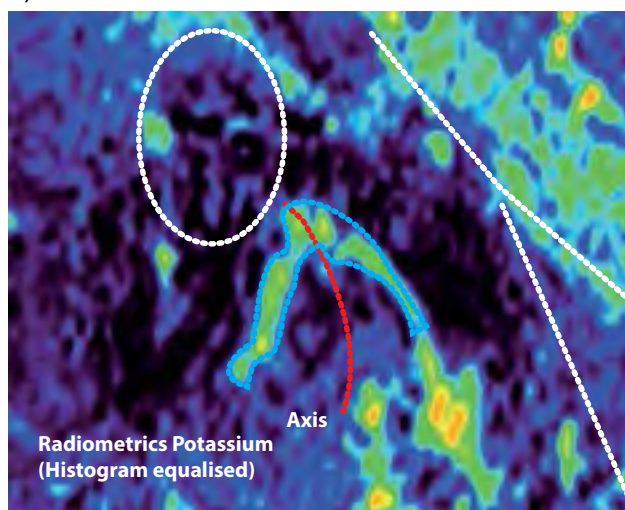
b)



c)



d)



0 10km

2014_04_0102

Figure 21. The Rock Hill and Flowerpot Hill area of Figure 20 (approx.) a) ASTER false colour; b) RTP TMI over Tilt-filtered TMI; c) Radiometrics: Ternary (RGB: K, Th, U); d) Radiometrics: K (blue: low; red: high). Major lineaments, magnetic low and fold structure are shown. NA = site not sampled in study.

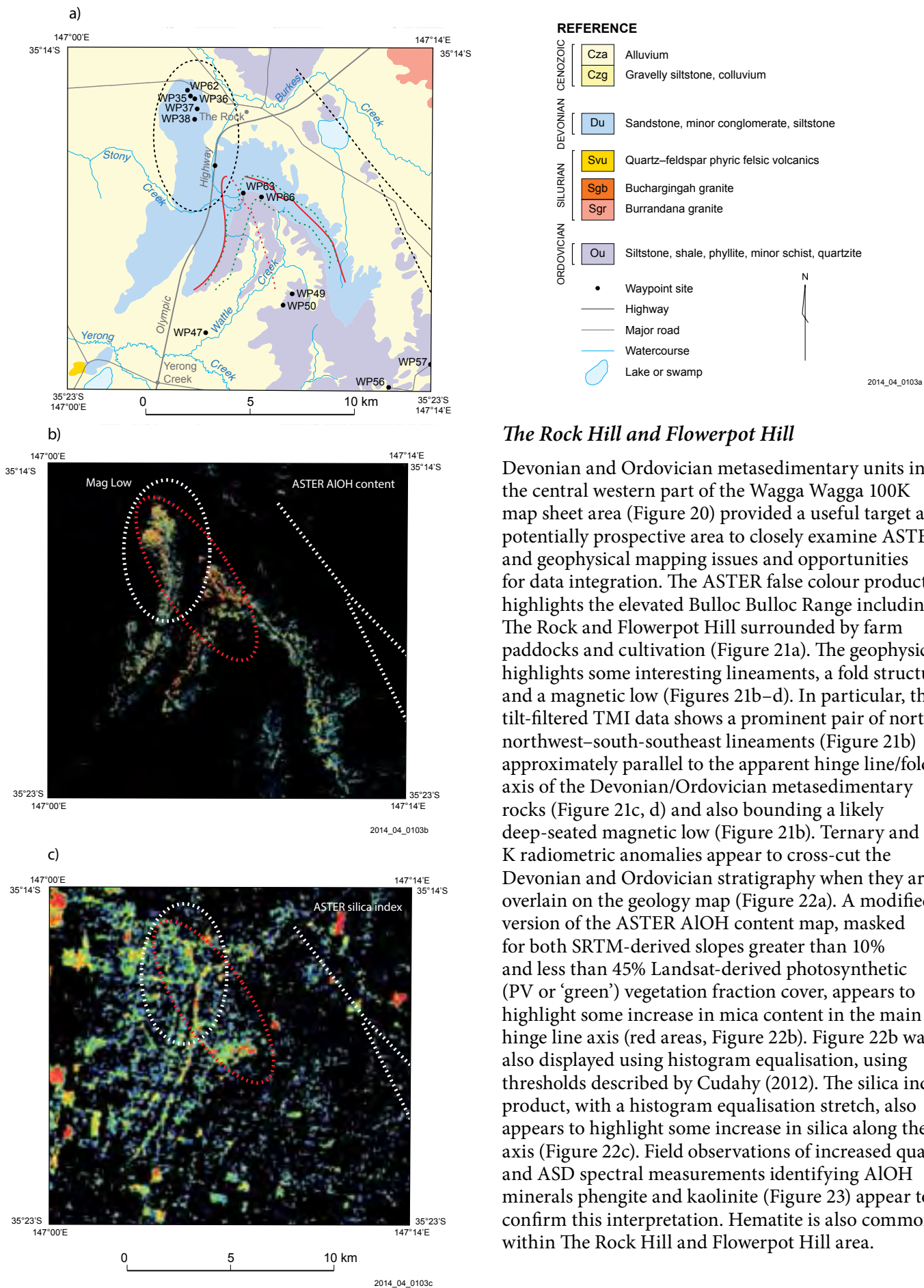


Figure 22. The Rock Hill and Flowerpot Hill. a) Wagga Wagga 100K geological map with geophysical features from Figure 21; b) ASTER AIOH masked for >10% slope and <45% PV Landsat fraction, histogram equalised. Mica anomaly is circled. c) ASTER silica index, histogram equalised. Silica anomaly is circled. Purple/blue: low to red: high content.

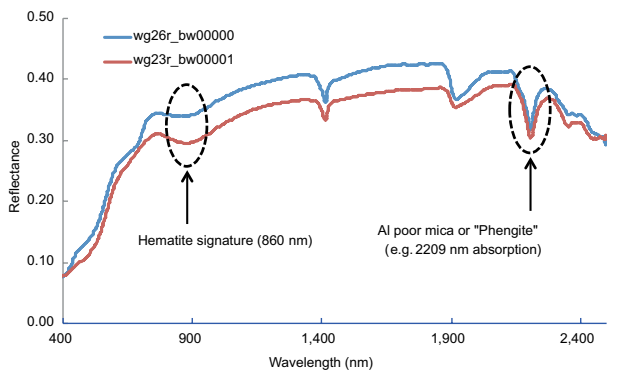
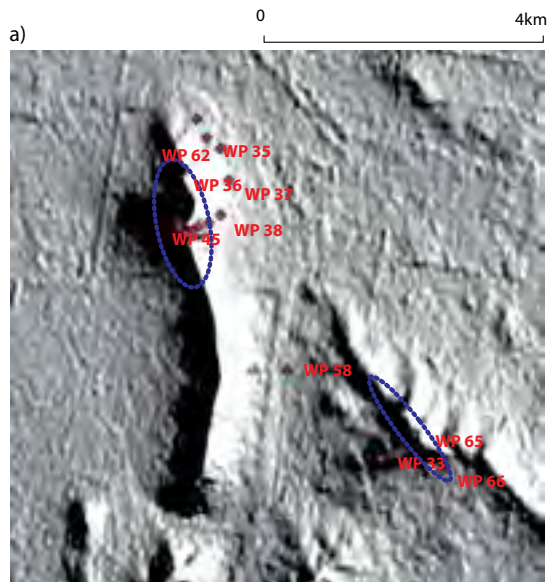


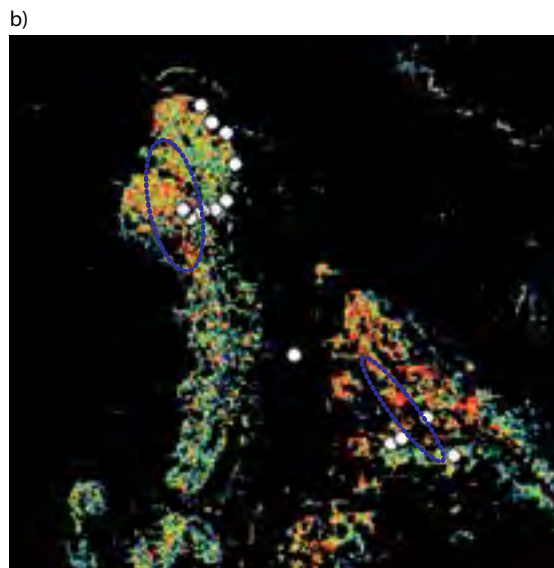
Figure 23. Example ASD spectral signature of rock outcrop samples (WG23, 26 – see Figure 21a) at Flowerpot Hill showing Al-poor mica/AIOH and hematite diagnostic features.

ASTER data issues and qualifications on interpretation

Acquisition of ASTER satellite imagery at about 10:30 am (Australian Eastern Daylight Time) can potentially produce sharp shadows on steep westerly slopes within high relief areas. The ASTER satellite sensor has an additional issue of potential false anomalies from the ‘crosstalk’ mis-calibration of its shortwave IR sensor (bands 5–9), as used for the generation of AIOH or mica/clay mineral maps. Dark shaded areas appear on the western slopes of The Rock and Flowerpot Hill as a result of north- and northwest-trending ridgelines, as shown in the sun-shaded DEM imagery generated to simulate illumination conditions on 11/1/2001 at 10:30 am (blue ellipses, Figure 24a). These areas of deep shadow appear to be coincident with some of the AIOH anomalies (red ellipse, Figure 22b) and potentially the result of false anomalies associated with crosstalk (Figure 24b). However, areas of full illumination on the northeast slopes also show AIOH anomalies and the crosstalk explanation does not entirely negate the AIOH presence. Overall these results suggest that residual crosstalk effects are a possibility within dark areas of shadow and vegetation cover and bitumen (e.g. the Wagga Airfield/RAAF base). The validation of ASTER study sites can be assisted with the aid of DEMs, fractional cover information, field observations and, ideally, a VNIR–SWIR spectrometer.



SRTM DEM sun shaded (el. 60°, Az 72°)



ASTER AIOH mica content (hist. eq.)
masked for 45% < green vegetation > 10% slope

Figure 24. a) Sun-shaded SRTM 80 m DEM of The Rock Hill and Flowerpot Hill (60° elevation, 072° azimuth), simulating illumination conditions and shaded relief during ASTER image acquisition (11/1/2001). b) ASTER AIOH content and corresponding areas of shaded relief (dashed ellipses).



Figure 25. The Rock Reserve, WP62, a) Casuarina open woodland; b) ferruginous gravel with lichen and moss ground cover; c) typical canopy cover.

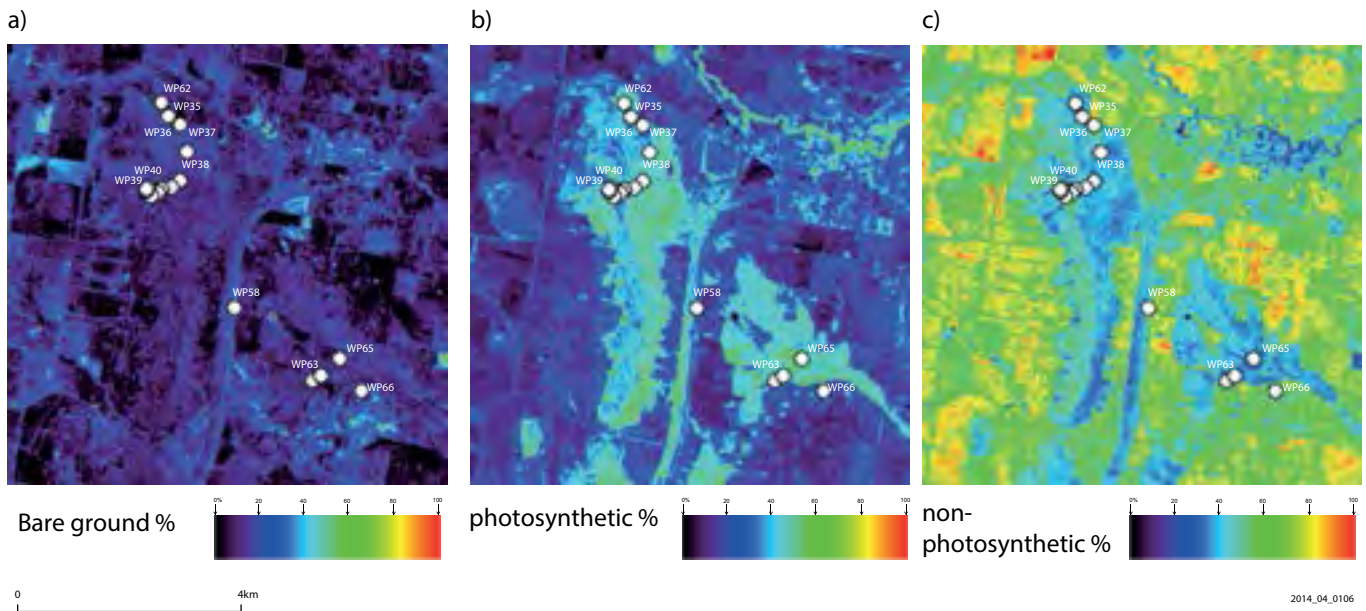


Figure 26. a) – c) Landsat fractional cover % estimates for The Rock Hill — the same area as in Figure 24.

Field observations and ASD in-situ field measurements of gravel lag, vegetation, ground litter etc at Waypoint WP62 (Figure 22a, 24a) were undertaken near The Rock (Figure 25a–c). AusCover fractional cover estimates, using Landsat acquired 10/1/2001, one day before the ASTER, gave values of 18% bare ground, 41% photosynthetic and 40% non-photosynthetic vegetation cover for supplied 30m pixels encompassing WP62. Fractional cover imagery for the Bullock Bullock Range/The Rock shows that the cover is dominated by photosynthetic, and to a lesser extent, non-photosynthetic vegetation (Figures 26a–c). ASD in-situ field measurements of gravel lag, vegetation, and ground litter at WP62 were processed to simulate ASTER ferric oxide content and green vegetation indices (Figure 27). This limited series of measurements suggested that the presence of dry vegetation matter (e.g. lichen, bark, leaf litter) can hinder the ASTER interpretation of ferric iron (e.g. hematite, goethite), useful for regolith profile information and/or alteration involving hematisation (Figure 27). Simulated values for ASTER’s AIOH content index from W62 gravel

lag ASD measurements produced values between 1.9 and 2.15, within the threshold range used to generate ASTER AIOH content imagery (Cudahy 2012). This compares favourably with the ASTER AIOH content index value of 2.0 as an average for 2 x 30 m pixels at WP62 extracted from the map product.

Cobar 1:100 000 and Canbelego 1:100 000 map sheet areas

The ASTER map products over the Cobar 1:250 000 map sheet area are less affected by agricultural cultivation than the Wagga Wagga area, as highlighted by ASTER’s false colour showing only approximately 25% under cultivation/cropping to the east (Figure 28a). Isolated cloud cover is also apparent in the eastern third of the Cobar 1:250 000 map sheet area, where the map product is generated from a separate ASTER scene (Figure 28a). ASTER’s regolith product is useful for highlighting the extensive ephemeral drainage patterns (Figure 28b). As described by Cudahy (2012), the Regolith product, based on the Landsat TM Regolith ratios, helps to separate regolith and geological units while vegetated areas are highlighted by white/bright areas, and clouds, in blue (Figure 28b). ASTER’s green vegetation product also shows the limited nature of the green vegetation cover, restricted to watercourses, outside of the cultivated areas (Figure 28c). The land cover is more explicitly highlighted in the Landsat-derived fractional cover image which shows that close to the time of ASTER acquisition (September 2003) the most exposed bare ground was within the Cobar 100K map sheet area, and to a lesser extent Canbelego 100K (reddish areas, Figure 28d). Non photosynthetic vegetation (‘dry vegetation’) still appears pervasive in the non-cultivated areas (blue areas, Figure 28d) which may be an issue for some ASTER map products.

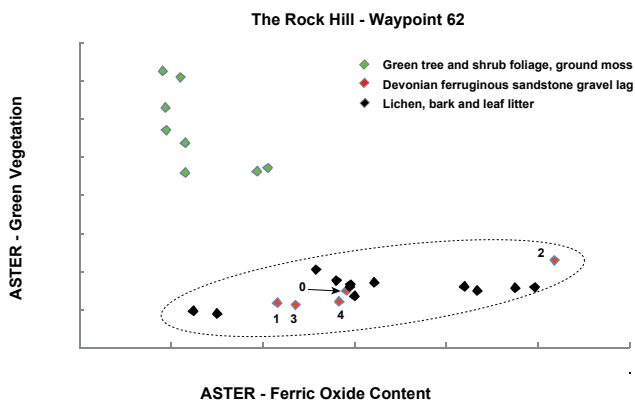


Figure 27. ASD field spectral signatures of vegetation and gravel samples from The Rock Hill (WP 62), resampled and processed into equivalent ASTER map indices for green vegetation and ferric oxide content.

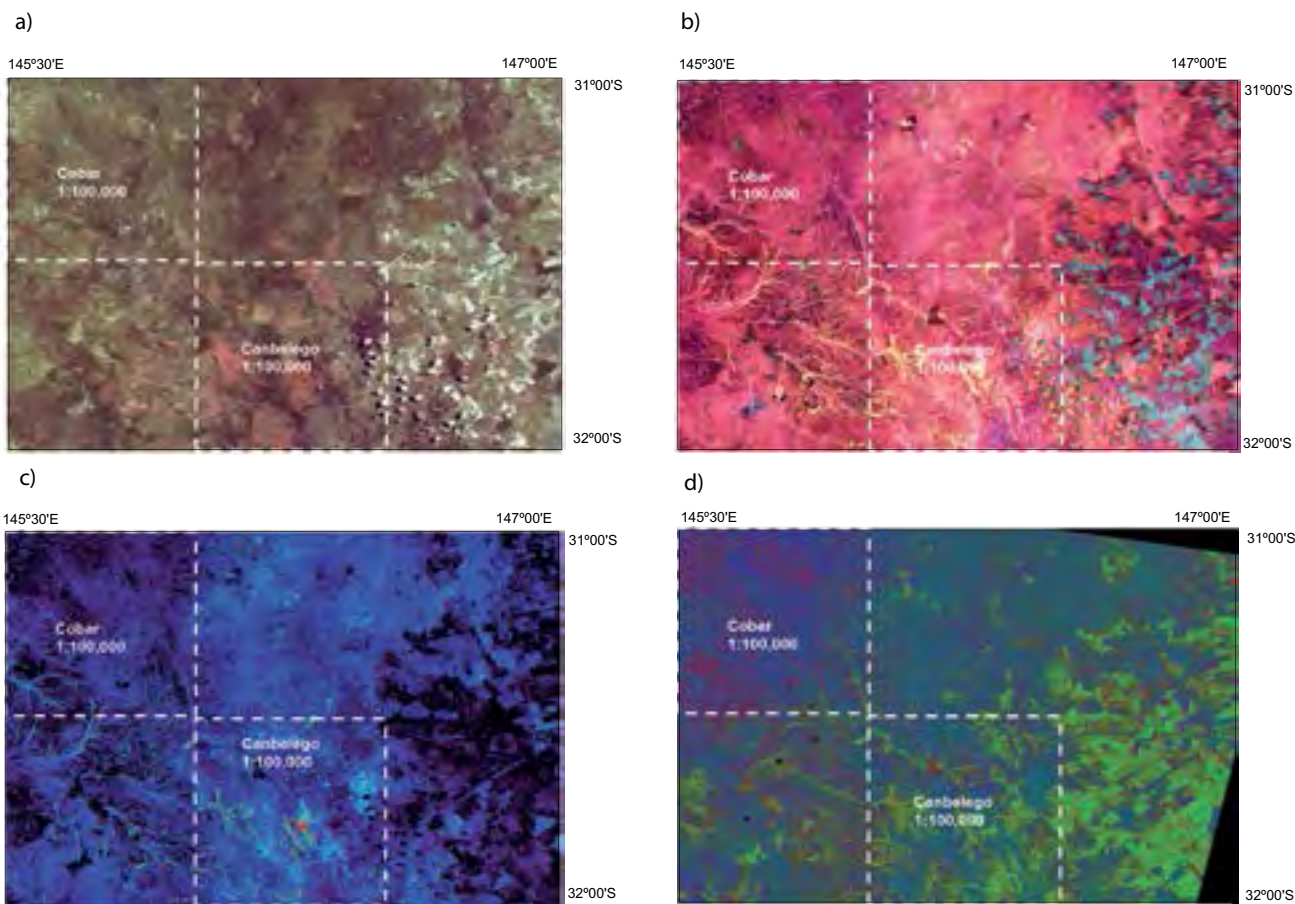


Figure 28. Cobar 1:250K map sheet area. a) ASTER false colour. Note clouds and shadows in lower right; b) ASTER regolith colour coded as for standard CSIRO Landsat Regolith product (Cudahy 2012); c) ASTER green vegetation (blue: low; red: high); d) Landsat fractional cover RGB. Red: bare ground, Green: photosynthetic vegetation, Blue: non-photosynthetic vegetation; (linear stretch, 0–100%).

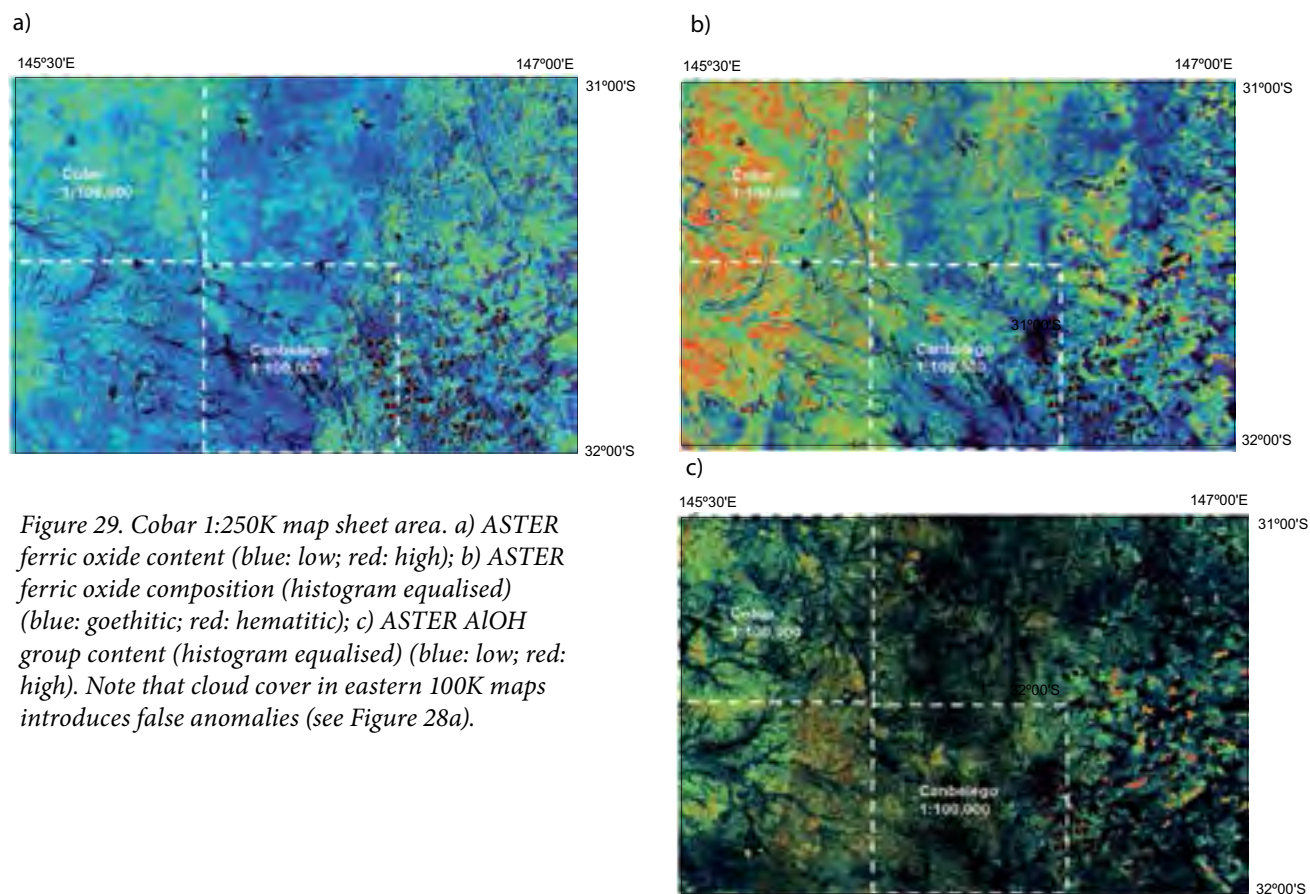


Figure 29. Cobar 1:250K map sheet area. a) ASTER ferric oxide content (blue: low; red: high); b) ASTER ferric oxide composition (histogram equalised) (blue: goethitic; red: hematitic); c) ASTER AIOH group content (histogram equalised) (blue: low; red: high). Note that cloud cover in eastern 100K maps introduces false anomalies (see Figure 28a).

2014_04_0109

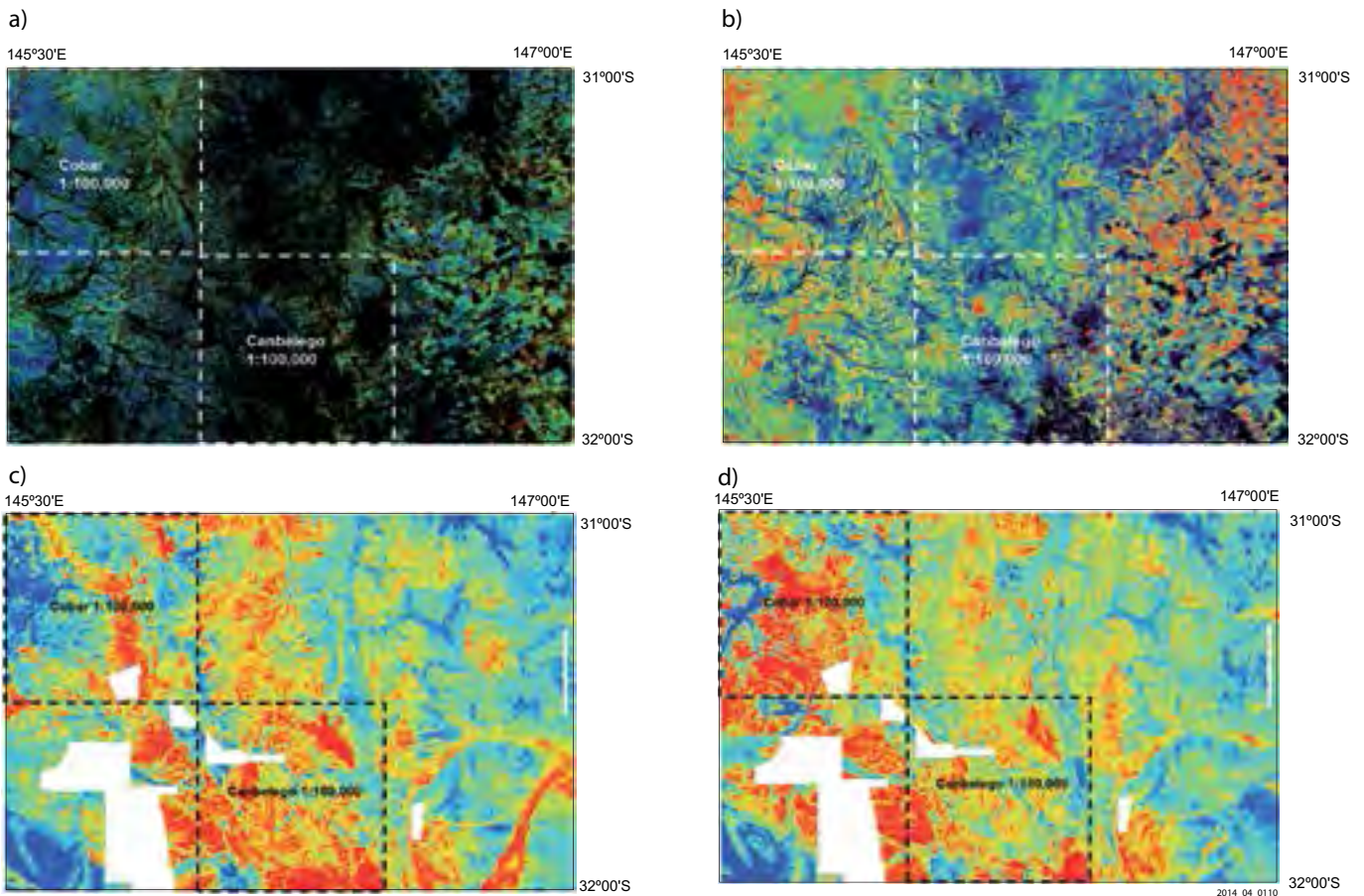


Figure 30. a) ASTER AIOH group composition (histogram equalised) (blue: Al-rich mica/well ordered kaolinite; red: Al-poor mica); b) ASTER silica index (histogram equalised) (blue: low; red: high); c) Radiometric K (blue: low; red: high); d) Radiometric Th (blue: low; red: high).

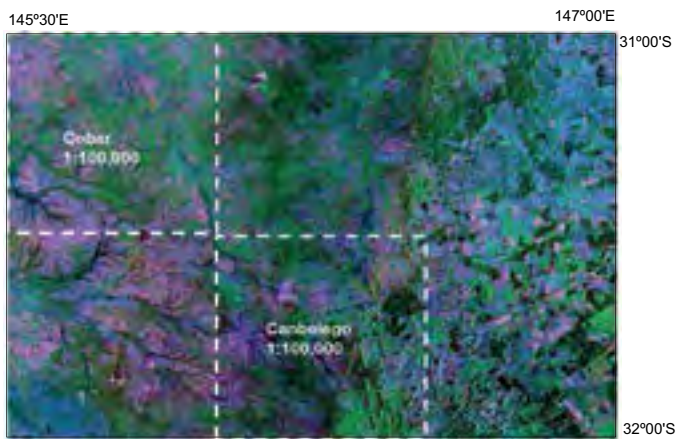
The ASTER Ferric Oxide Content product highlights coherent and continuous spatial distribution across the Cobar 1:250 000 sheet area, with increased abundance within the Cobar 100K area (Figure 29a). An improved insight into the ferric iron oxide was provided by the ASTER's ferric oxide composition using histogram equalisation (Figure 29b), rather than a Gaussian stretch, within the same threshold stretch limits advised by Cudahy (2012). Using the histogram equalised version of the ASTER ferric oxide composition product highlights more clearly an apparent increase in hematitic composition within the western Cobar 250K, including the Cobar 100K map sheet area (Figure 29b). The presence of hematite versus goethite may be important for regolith interpretation and understanding of the area's possible lateritic weathering (Huntington et al. 1999). However, care should also be taken when interpreting ferric oxide content and composition in the presence of dry vegetation matter — as observed at The Rock Hill (Figure 27) and also noted by Cudahy (2012). The areas highlighted by ASTER with increased hematite also coincide with increased abundance of AIOH minerals, as shown by the histogram equalised version of the ASTER AIOH group content (green–yellow areas, Figure 29c).

The ASTER AIOH group composition product (histogram equalised, Figure 30a) highlights extensive

areas of low values (blue) in the western Cobar 250K sheet area, including within the Cobar 100K. Cudahy (2012) interpreted such low ASTER AIOH composition product values as mapping well-ordered kaolinite or Al-rich white mica. These areas also appear to coincide with the interpreted hematite-rich areas shown in Figure 29b (red areas). If a lateritic profile mineral model (Huntington et al. 1999) is assumed then questions arise whether these areas lie within the highly weathered hematite-bearing duricrust or less-weathered, ordered kaolinite-bearing saprolite. The ASTER kaolin group index product for Cobar 250K sheet area does not indicate significant anomalies, using linear or histogram equalised versions. Cobar regolith landform mapping indicates much of the Cobar 100K area is highly weathered in situ bedrock (Gibson 1999). However, validation field work involving sampling and ASD measurements should clarify these issues.

The ASTER silica index product does appear to indicate high silica content along the western boundary of the Cobar 100K sheet area that coincides with elevated areas mapped by Gibson (1999) containing cappings of silicified sedimentary units (histogram equalised, Figure 30b). Geophysical radiometric products K and Th also highlight distinctive units with the Cobar 100K and Canbelego 100K map sheet areas (Figures 30c, d). The K and Th images mostly appear to map, in an approximate complementary way, areas of alluvial

a)



b)

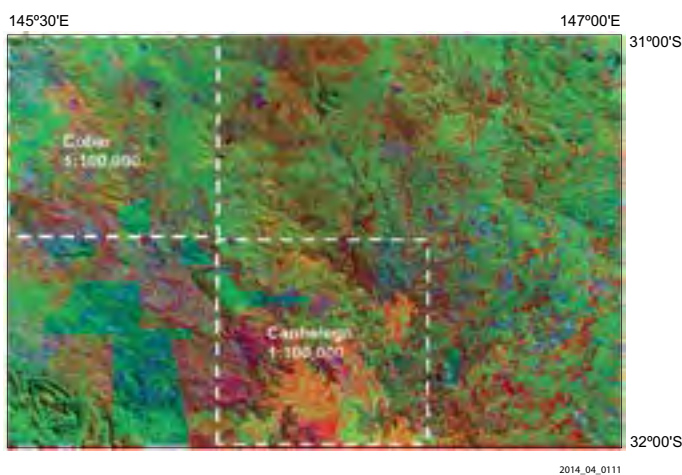


Figure 31. a) RGB composite: ASTER's AIOH content (histogram equalised), ferric oxide content, silica index (histogram equalised); b) RGB composite: K, ASTER's ferric oxide content, AIOH content over shaded DEM.

(e.g. K) and in situ regolith units (e.g. Th) (Figures 30c, d). In particular the drainage areas appear rich in apparently K-bearing clays (Figure 30c) whilst the Th occurs where there are non-drainage in situ relict areas (Figure 30c), possibly related to ferricrete. Further ground truthing would help this interpretation.

An RGB composite image of ASTER's AIOH group content, ferric oxide content and silica index products appeared to discriminate generally elevated combined clay- and quartz-rich units (e.g. red+blue areas shown as purple) from ferric iron oxide minerals (green) within some drainage areas (Figure 31a). A RGB composite image of the radioelement K, ASTER ferric oxide content and ASTER AIOH group content products also generated significant and complex spatially coherent patterns, particularly within the Cobar and Canbelego 100K sheet areas, that appear worthy of further examination for regolith information (Figure 31b).

Conclusions

This project demonstrated, within the NSW study areas of Wagga Wagga and Cobar, the usefulness of the recently released Australia ASTER map products supplied by CSIRO/GA for identifying or discriminating variations in surface composition. The map products included mineral identities/groups within geological units, possible overprinted alteration and/or weathered regolith. These map products can potentially aid mineral exploration in NSW within semi-arid areas such as Cobar and, to a lesser extent, within open woodland and cultivated environments such as Wagga Wagga. Although several ASTER map products provided useful information as individual entities, their application generally benefits exploration when integrated with geophysical, topographical and fractional land cover information. In particular, DEM-derived slope information and vegetation fractional data were used to mask and refine ASTER map products in the Wagga area within the temperate and vegetated Riverine Plains. Anomalous AIOH- and silica-rich areas were discriminated and associated with radiometric and high frequency filtered TMI-inferred structures in the vicinity of the Bullock Bullock Range, especially at The Rock Hill. ASTER Ferric Iron Content product within the Wagga Wagga area also appeared to show northwest lineament trends similar to those highlighted by filtered TMI products. Map generation for the Murrumbidgee floodplains using radiometric data also appeared to benefit from topographic slope masking to exclude areas of alluvial and aeolian transported cover.

More spatially coherent anomalous areas, particularly related to the regolith, were identified by the ASTER map products in the semi-arid and rangeland terrain of Cobar. The application of different histogram stretches, such as histogram equalisation, was found to further enhance the display of anomalous features — although care should be applied regarding data thresholds. The application of the ASTER map products individually, as RGB composites, or integrated with radiometric data, appears useful for regolith mapping and identifying weathering profile-related mineralogy at Cobar.

Effects of residual ASTER crosstalk mis-calibration within areas of shadow/dark surfaces/dense vegetation, and possible interpretation ambiguities between VNIR-derived ferric oxide and dry vegetation, highlight the importance of validation fieldwork to check anomalous areas and their spectral signatures. The validation of ASTER study sites may be assisted by DEM and fractional cover information. Further investigations into the benefits of integrating artificially illuminated, shaded topographic relief and AusCover fractional land cover information, relevant for ASTER acquisition dates, are recommended.

Acknowledgements

This study has been supported and funded by the Geological Survey of New South Wales, in part, for the purpose of contributing to the knowledge of the Wagga Wagga 1:100 000 map sheet geology for mineral exploration. Geophysical and associated data for the Wagga Wagga and Cobar study areas were received from the Geological Survey of New South Wales. ASTER GeoTIFFs and BSQ ASTER map products were also gratefully obtained from Geoscience Australia and CSIRO–Earth Science & Resource Engineering, whilst the original ASTER imagery was made available by NASA and METI. GIS shapefiles for the Wagga Wagga and Cobar 1:250 000 map sheet areas were also gratefully obtained from Geoscience Australia. Assistance is also gratefully acknowledged from Thomas Cuday and Carsten Laukamp of CSIRO, and Matilda Thomas of Geoscience Australia. Support from Professor Simon Jones and Laurie Buxton of RMIT University was also helpful during this study.

References

CACETTA M., COLLINGS S. & CUDAHY C. 2013. A calibration methodology for continental scale mapping using ASTER imagery, *Remote Sensing of Environment* **139**, 306–317.

CHAN R.A., GREENE R.S.B., DE SOUZA KOVACS N., MALY B.E.R., MCQUEEN K.G., & SCOTT K.M. 2003. Regolith, geomorphology, geochemistry and mineralisation of the Sussex–Coolabah area in the Cobar–Girilambone region, North-Western Lachlan Foldbelt, NSW, CRC LEME openfile report 148 / NSW DMR Report GS2001/319.

CHEN X.Y. 1997. Quaternary sedimentation, parna, landforms, and soil landscapes of the Wagga Wagga 1:100 000 map sheet, south-eastern Australia, *Australian Journal of Soil Research*, **35(3)**, 643–668.

CHEN X.Y. & MCKANE D.J. 1997. *Soil Landscapes of the Wagga Wagga 100K Sheet map and report*, Department of Land and Water Conservation, Sydney.

CLARK R.N., KING T.V.V., KLEJWA M., SWAYZE G.A. & VERGO N. 1990. High spectral resolution reflectance spectroscopy of minerals. *Journal of Geophysical Research* **95(B8)**, 12653–12680.

CUDAHY T.J. 1997. *PIMA-II spectral characteristics of natural kaolins*. CSIRO Exploration and Mining, Report 420R, 57 pp.

CUDAHY T.J. 2012. *Satellite ASTER Geoscience Product Notes for Australia*, Version 1, 7th August, 2012. CSIRO, ePublish No. EP-30-07-12-44.

DOWNES P.M., MCEVILLY R. & RAPHAEL N.M. 2004. Mineral deposits and models, Cootamundra 1:250 000 map sheet area. *Quarterly Notes of the Geological Survey of New South Wales* **116**, 1–38.

DOWNES P.M. & SECCOMBE P.K. 2008. Sulfur isotope signatures for orogenic gold deposits, Lachlan Orogen, New South Wales. In: *Proceedings of PACRIM Congress, 24–26 November, 2008, AusIMM, Gold Coast, Queensland, Australia*.

DUKE E.F. 1994. Near infrared spectra of muscovite. Tschermak substitution and metamorphic reaction process: implications for remote sensing. *Geology* **22**, 621–624.

GIBSON D.L. 1999. *Explanatory notes for the 1:500 000 Cobar regolith landform map*, CRC LEME / Geological Survey of NSW, Open File Report 76.

GROVE C.I., HOOK S.J. & PAYLOR E.D. III 1992. *Laboratory reflectance spectra of 160 minerals, 0.4 to 2.5 micrometers*. NASA Jet Propulsion Laboratory report JPL Publication 92-2.

HEWSON R. 2013. *Using ASTER and geophysical mapping to assist exploration over Wagga Wagga 1:100 000 sheet area*. Geological Survey of New South Wales, File GS2013/1558.

HEWSON R.D. & CUDAHY T.J. 2011. Issues Affecting Geological Mapping with ASTER Data: A Case Study of the Mt Fitton Area, South Australia. In: Ramachandran B., Justice C.O. & Abrahams M.J. (eds) *Land Remote Sensing and Global Environmental Change: NASA's Earth Observing System and the Science of ASTER and MODIS: Applications in ASTER*, pp. 273–300. Springer-Verlag, New York

HEWSON R.D., CUDAHY T.J., DRAKE-BROCKMAN J., MEYERS. J. & HASHEMI A. 2006. Mapping geology associated with manganese mineralization using spectral sensing techniques at Woodie Woodie, East Pilbara, *Exploration Geophysics* **37**, 389–400.

HEWSON R.D., CUDAHY T.J. & HUNTINGTON J.F. 2001. Geologic and alteration mapping at Mt Fitton, South Australia, using ASTER satellite-borne data. In: *Geoscience and Remote Sensing Symposium, 2001. IGARSS '01. IEEE 2001 International*, vol.2, 724–726.


- HEWSON R.D., CUDAHY T.J., MIZUHIKO S., UEDA K. & MAUGER A.J. 2005. Seamless geological map generation using ASTER in the Broken Hill–Curnamona Province of Australia. *Remote Sensing of Environment* **99**(1–2), 159–172.
- HEWSON R.D., MAH A., DUNNE M. & CUDAHY T.J. 2003. Mapping mineralogical and structural relationships with satellite-borne ASTER and airborne geophysics at Broken Hill. ASEG 16th Geophysical Conference and Exhibition, Adelaide, February 2003. Australian Society Exploration Geophysicists.
- HEWSON R., ROBSON D., MAUGER A., CUDAHY T., THOMAS M. & JONES S. 2013. Extracting mineralogical and geomorphological information using new ASTER mineral maps with airborne geophysics. *Proceedings of the ASEG–PESA 2013, 23rd International Geophysical Conference and Exhibition, 11–14 August 2013, Melbourne, Australia*.
- HUNT G.R. & ASHLEY R.P. 1979. Spectra of altered rocks in the visible and near infrared. *Economic Geology*, **74**, 1613–1629.
- HUNTINGTON J.F., CUDAHY T.J., YANG K., SCOTT K.M., MASON P., GRAY D.J., BERMAN M., BISCHOF L., RESTON M. S., MAUGER A.J. KEELING J.L. & PHILLIPS R.N. 1999. *Mineral mapping with field spectroscopy for exploration – final report*. CSIRO/AMIRA Project P435. CSIRO Exploration and Mining, Report 419R.
- IWASAKI A., FUJISADA H., AKAO H., SHINDOU O. & AKAGI S. 2001. Enhancement of spectral separation performance for ASTER/SWIR. *Proceedings of SPIE (International Society for Optical Engineering)*, **4486**, 42–50.
- IWASAKI A. & TONOOKA H. 2005. Validation of a crosstalk correction algorithm for ASTER/SWIR. *IEEE Transactions on Geoscience and Remote Sensing*, **43**(12), 2747–2751.
- LAUKAMP C., CUDAHY C., CACCETTA M., THOMAS M., CLOSE D. & LENNARTZ R. 2013. Successful mineral exploration using multispectral remote sensing data – ASTER Geoscience Map of Australia, *In: Proceedings, 12th Biennial Meeting of the Society of Geology Applied to Mineral Deposits (SGA)*. Uppsala, Sweden, 12–15 August 2013.
- LEWIS P. & DOWNES P.M. 2008. Mineral systems and processes in New South Wales: a project to enhance understanding and assist exploration, *Quarterly Notes of the Geological Survey of New South Wales* **128**.
- MCQUEEN K.G. 2008. *A guide for mineral exploration through the regolith in the Cobar Region, Lachlan Orogen, New South Wales*. Cooperative Research Centre for Landscape Environments and Mineral Exploration.
- MICHAEL S. 2012. Satellite imagery: the range and value. CSIRO Publishing for Australian Society for Exploration Geophysicists. *Preview* 2012(**160**), 20–25.
- RAYMOND O. 1993. Wagga Wagga–Kyeamba region geological map 1:100 000. Australian Geological Survey Organisation, Canberra.
- RICCHETTI E. 2000. Multispectral satellite image and ancillary data integration for geological classification. *Photogrammetric Engineering & Remote Sensing* **66**(4), 429–435.
- ROWAN L.C. & MARS J.C. 2003. Lithologic mapping in the Mountain Pass, California area using Advanced Spaceborne Thermal Emission and Reflection Radiometer (ASTER) data. *Remote Sensing of Environment* **84**, 350–366.
- SALISBURY J.W. & D'ARIA D.M. 1992. Emissivity of terrestrial materials in the 8–14 μm atmospheric window. *Remote Sensing of Environment* **42**, 83–106.
- SCARTH P., RÖDER A. & SCHMIDT M. 2010. Tracking grazing pressure and climate interaction – the role of Landsat fractional cover in time series analysis. *In: Proceedings of the 15th Australasian Remote Sensing and Photogrammetry Conference (ARSPC)*, 13–17 September, Alice Springs, Australia.
- SHERMAN D.M. 1985. The electronic structures of Fe³⁺ coordination sites in iron oxides: application to spectra, bonding and magnetism. *Physics and Chemistry of Minerals* **12**, 161–175.
- VINCENT R.K. & THOMSON F. 1972. Spectral compositional imaging of silicate rocks. *Journal of Geophysical Research* **77**(14), 2465–2472.
- YAMAGUCHI Y., FUJISADA H., KAHLE A., TSU H., KATO M., WATANABE H., SATO I., & KUDOH M. 2001. ASTER instrument performance, operation status, and application to earth sciences. *In Geoscience and Remote Sensing Symposium, 2001. IGARSS '01. IEEE 2001 International*, vol.3, 1215–1216.

PRODUCT ORDER FORM

All prices are in Australian dollars and include Goods and Services Tax at 10%, unless otherwise noted. Only Australian orders are subject to the GST and all international orders will be processed exclusive of GST. All totals will be billed in Australian Dollars. International customers will be charged the equivalent of this rate in their respective currencies at the time the bank processes the transaction.

Item	Price (incl. GST)	Quantity	Line Total

Postage: Domestic \$8 (1-2 items) \$10 (3-5 items) \$12 (5+ items) Express \$13 | International \$45 (excl. GST)

 Be sure to select international postage above if you are an overseas customer. **Subtotal** (excl. GST for internationals)

Credit card surcharge: MasterCard 0.4% Visa 0.4% AMEX 1.5% Diners Club 2.4% | Other payment (N/A)

TOTAL

OFFICE
USE
ONLY

SHIPPING/CONTACT

Please note that we cannot ship to PO boxes.

FULL NAME		JOB TITLE	
STREET ADDRESS		ORGANISATION	
CITY, STATE	POSTCODE	COUNTRY	
PHONE	EMAIL		

PAYMENT




We accept payment by credit card, cheque, or money order (made payable to NSW Department of Trade & Investment).



CARD NUMBER				NAME ON CARD			
EXPIRY	SECURITY CODE	CARDHOLDER SIGNATURE	DATE				

RETURN

 Information and Customer Service Centre
NSW Department of Trade & Investment
PO Box 344, Hunter Region Mail Centre NSW 2310

 mineralpublication.orders@industry.nsw.gov.au
 +61 2 4931 6700  Enquiries: +61 2 4931 6666

Did you know? Selected products can be purchased from the NSW Government Online Shop: www.shop.nsw.gov.au

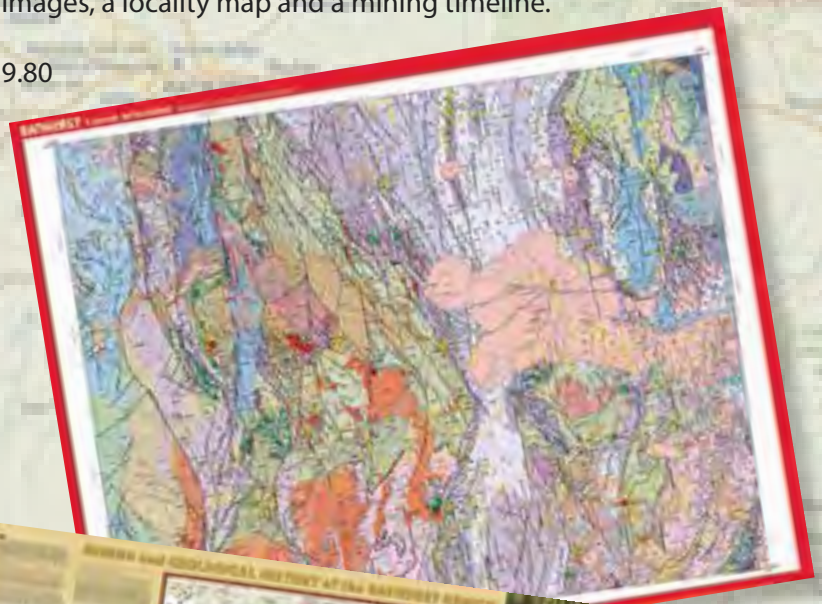


Second edition Bathurst metallogenic 1:250 000 map

Replacing the popular 1972 edition, the updated map shows 311 metallic, industrial, construction material and fuel deposits classified by size, commodity and deposit type. A deposit classification scheme is included, along with a time-space plot showing major mineralising events.

On the back of the map is a comprehensive poster summarising the mining history and geological history of the area. It features many colourful and historic images, a locality map and a mining timeline.

Cost: \$19.80



**Trade &
Investment**
Resources & Energy

NSW Trade & Investment, Division of Resources & Energy
516 High Street, Maitland NSW 2320
PO Box 344 Hunter Region Mail Centre NSW 2310
T:1300 736 122 T: (02) 49316666

www.resources.nsw.gov.au